

# From pattern formation to nonequilibrium distributions in mixtures of different mass fermionic ultracold atoms in optical lattices

J. K. Freericks

Department of Physics

Georgetown University

*Funding from NSF, ONR and DARPA*



*Supercomputer time from a DOD CAP and a NASA NLCS allocation*

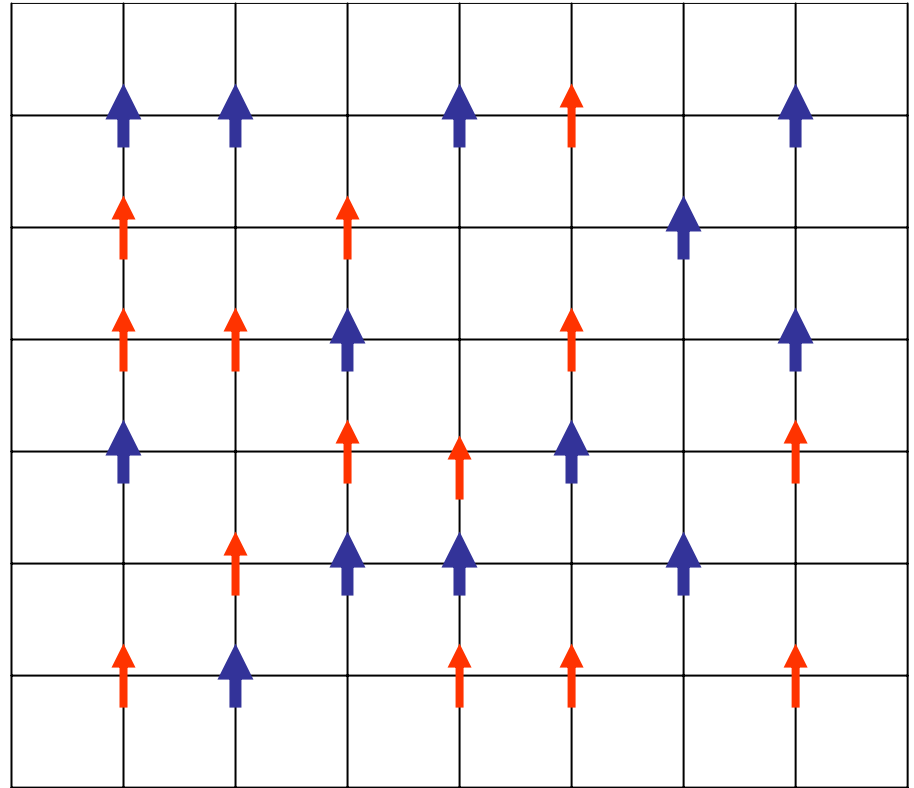
Thanks to Sasha Joura, Romuald Lemanski, Maciej Maska, Volodmyr Turkowski, Carl Williams, and Veljko Zlatic' for collaborating on this work.

# Mixtures of different mass atoms in an inhomogeneous trap on a two-dimensional square lattice

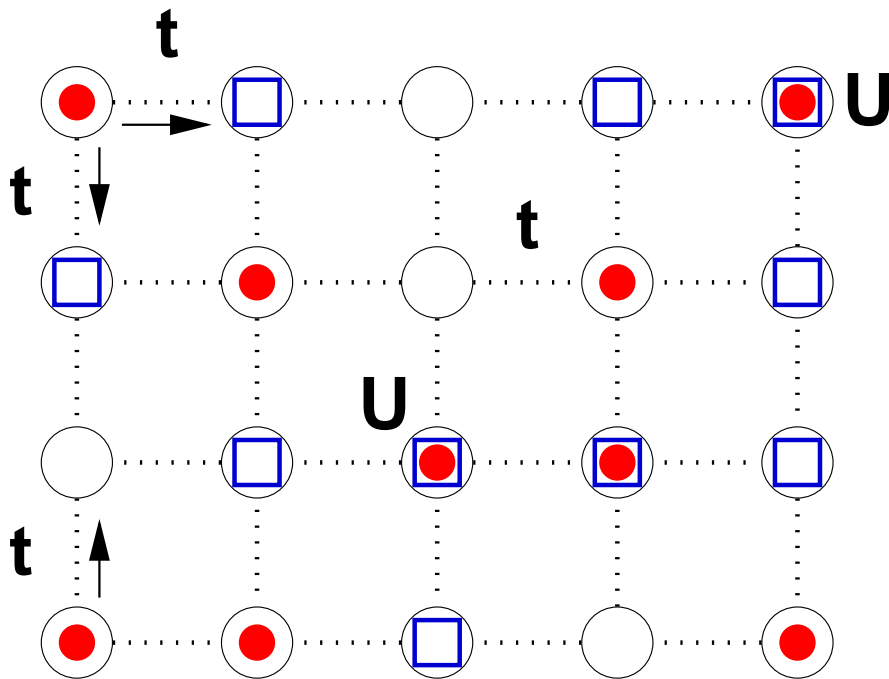


# Spin polarized heavy and light fermionic atoms on an optical lattice

- Heavy atoms (Sr or Yb)
- Light atoms (Li or K)
- Optical trap to allow different trapping frequencies for each species.



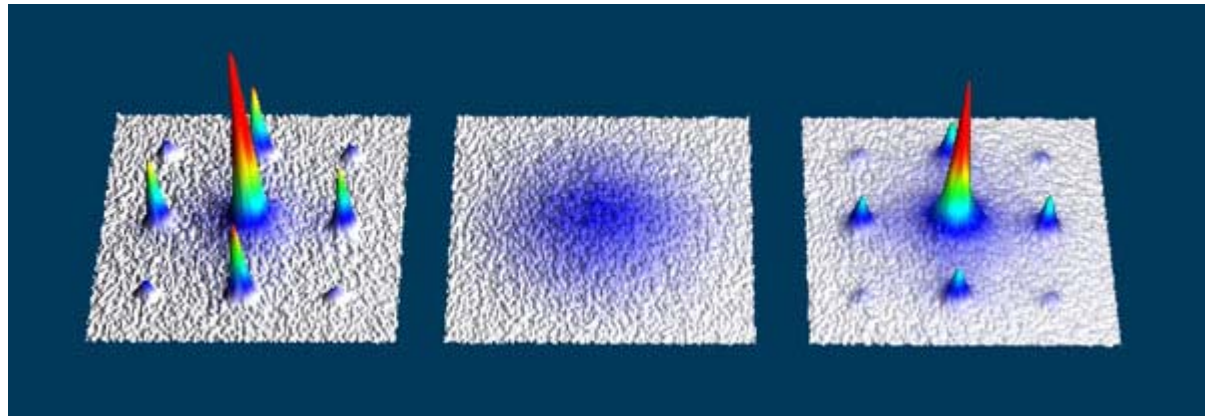
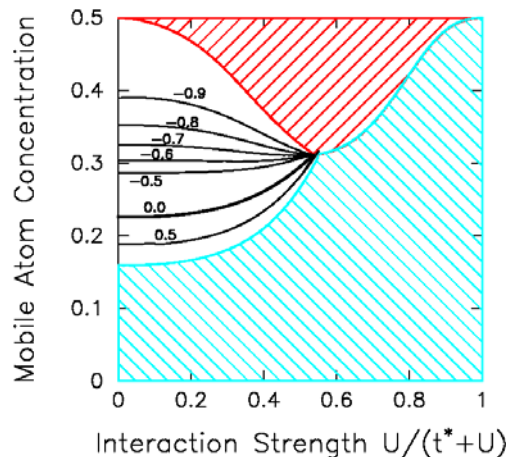
# Falicov-Kimball Model



- Two kinds of particles: (i) **mobile atoms** and (ii) **localized atoms**.
- When both atoms are on **the same site** they interact with a correlation energy  $U$ .
- Work on a 50x50 square lattice and keep  $\omega_H=1/30$  fixed, but vary  $\omega_L$ .
- Keep 625 heavy and 625 light atoms in the lattice.

# Physical importance of the Falicov-Kimball Model

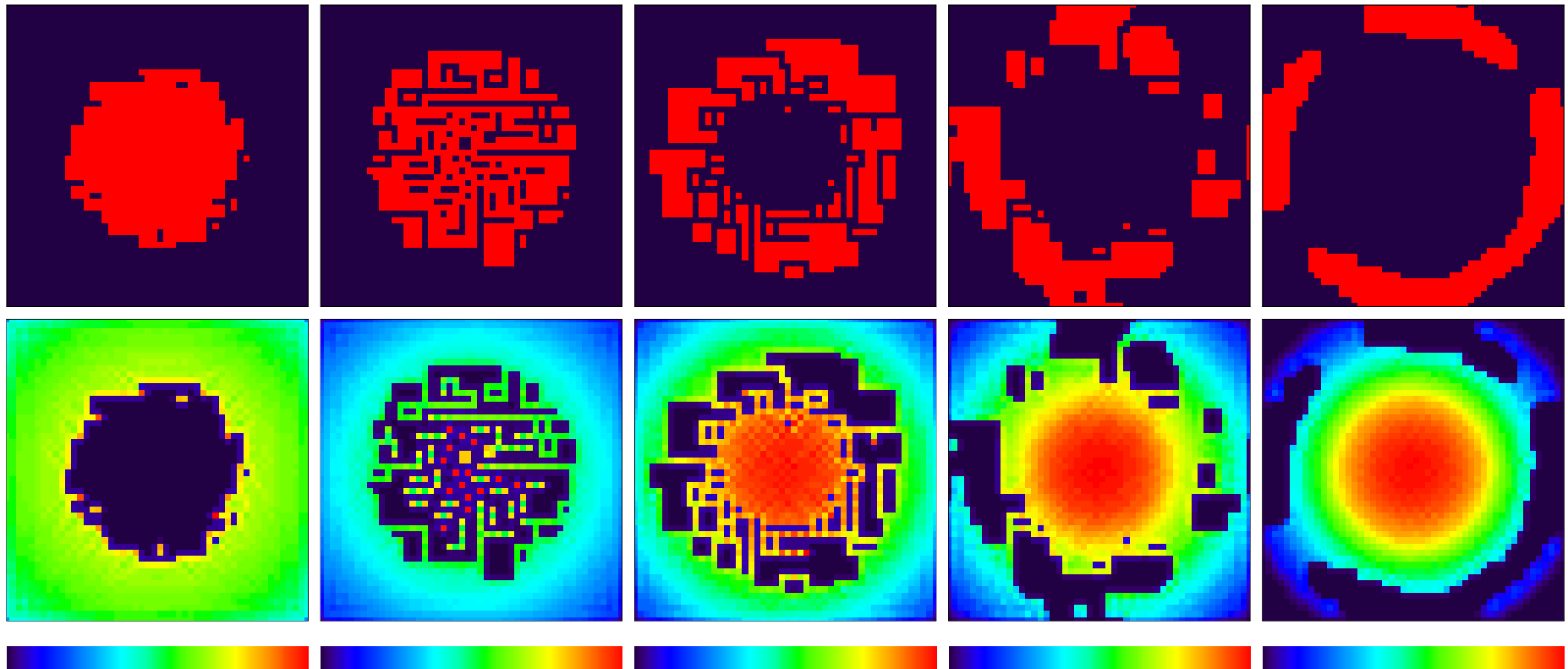
- Simplest many-body problem that has a Mott-like metal-insulator transition (but it has no Fermi-liquid behavior).
- Possible cold atom systems include mixtures of light alkali atoms (Li or K), with heavy atoms (Sr or Yb) in optical lattices.
- Possible solid-state systems include  $\text{NiI}_2$  and  $\text{Ta}_x\text{N}$



# Possible realizations of the FK model in cold atoms

- Each experimental measurement is like a QMC “snapshot” with the configuration chosen according to the equilibrium probability distribution.
- The heavy atoms are not fully localized but the quantum effects of their kinetic energy can be ignored, approximating the annealed averaging of the FK model.

# Two-d QMC simulation results ( $U=5$ )

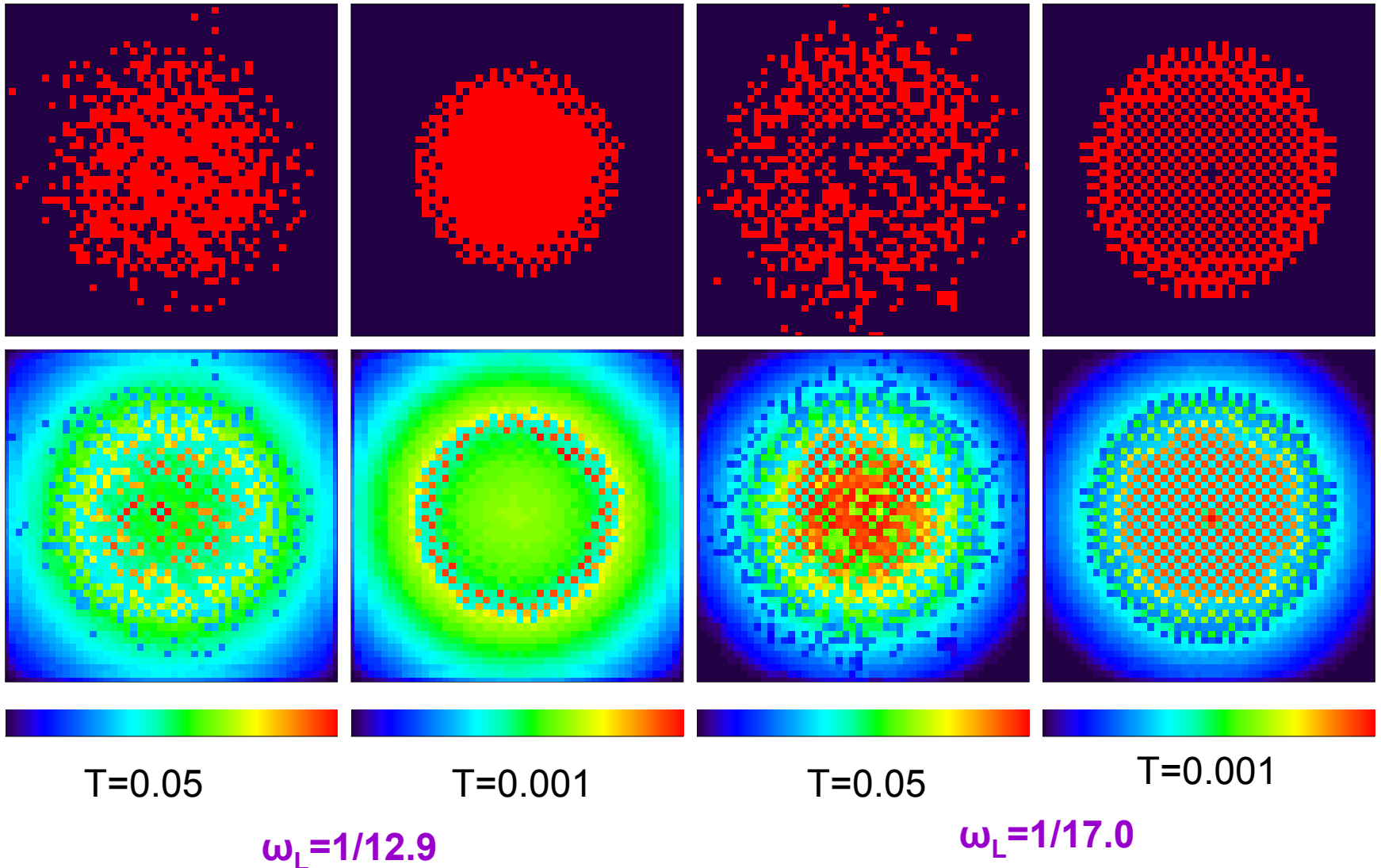


Top, heavy atom density (red) and bottom, light atom density  
The trap for the lights sharpens from left to right. The QMC  
snapshot is the analog of a cold-atom imaging experiment.

# Viscous fingering, labyrinthine patterns, and stripes

The system has a strong tendency to phase separate. The viscous fingering-like arrangement of the atoms as one atomic species is squeezed relative to the other (via changing the trap frequency) occurs because *axial stripe phases* are stabilized in the intermediate regime, which create the fingering effect, and results solely from the inhomogeneity. The specific patterns appear similar to the labyrinthine patterns in ferrofluids.

# Two-d QMC simulation results ( $U=1$ )



# Ordered pattern formation

For weaker coupling ( $U=1$ ), the system can form a number of different ordered phases, like the checkerboard phase, or higher period phases, in addition to the phase separation.

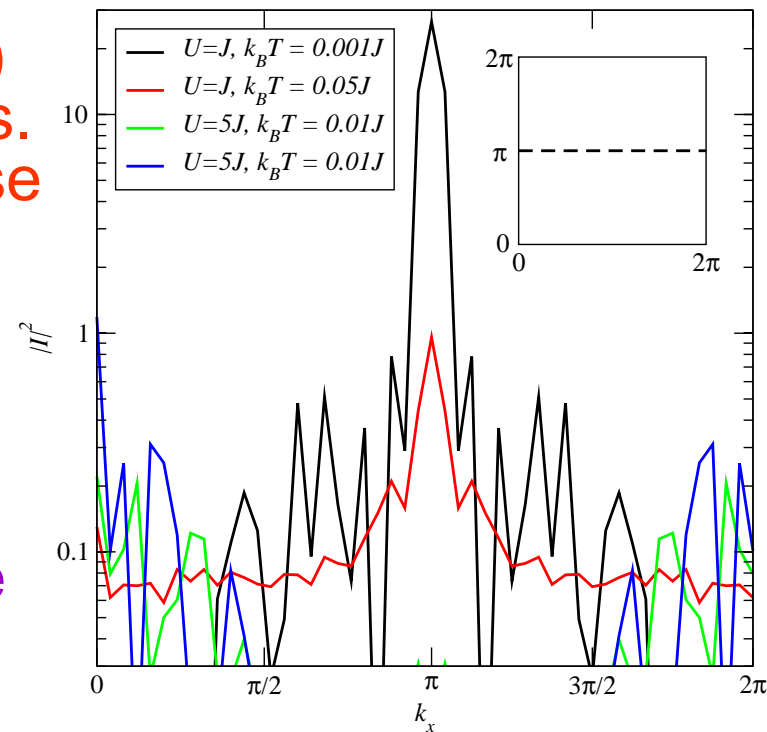
The ordering temperature can be fairly low though.



# Measurement of the patterns

*Bragg diffraction:* Look for peaks appearing at  $(\pi, \pi)$  for the checkerboard phase, and at  $(\pi, 0)$  or  $(0, \pi)$  for the axial stripe phases. If these peaks rise above the noise floor, one can image the pattern formation.

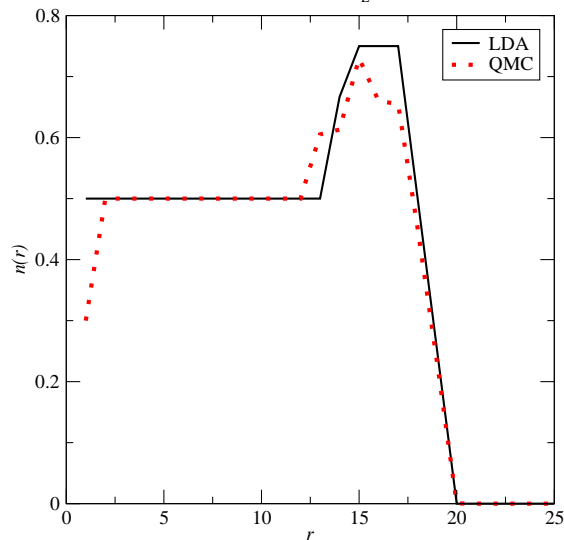
*Noise-correlation spectroscopy:* By examining the shot-to-shot noise of a time-of-flight experiment, one can measure density-density correlation functions which will exhibit peaks at the same momentum points when the pattern formation has occurred.



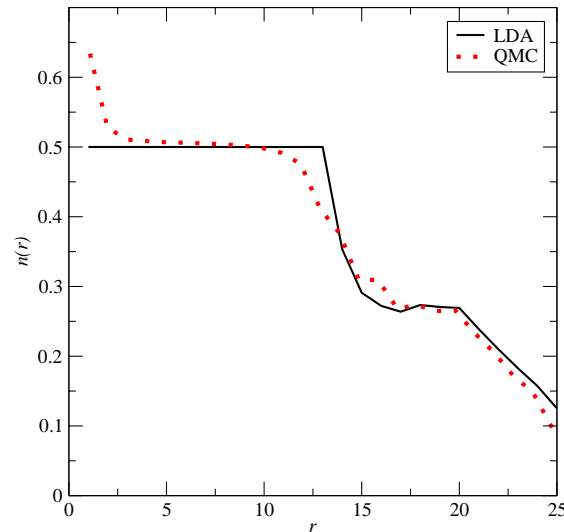
# Local density approximation

# Two-d local density approximation

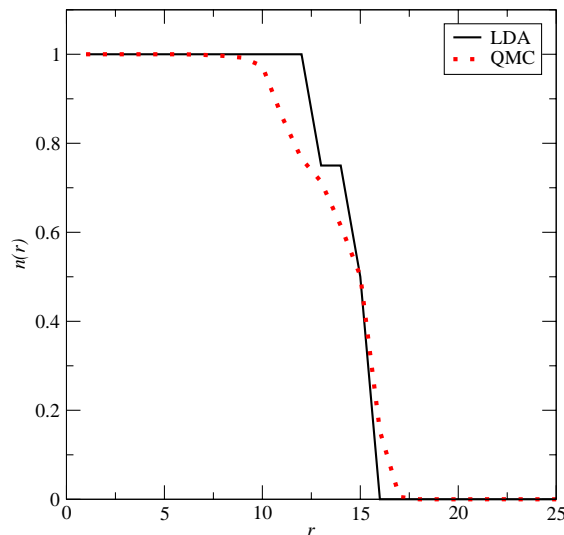
HEAVY ATOMS,  $R_L = 12.9a$



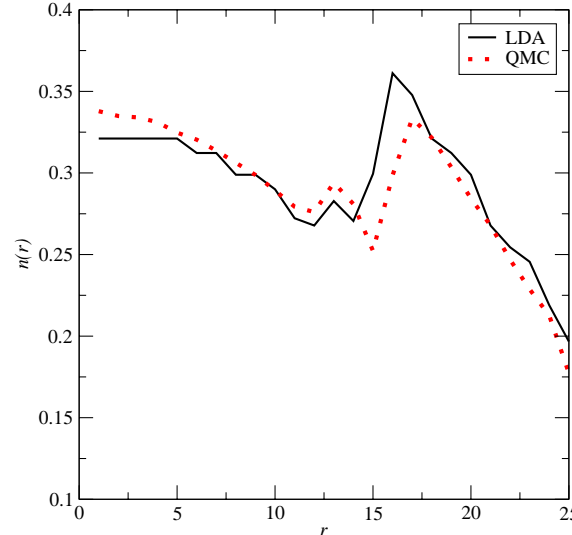
LIGHT ATOMS,  $R_L = 12.9a$



HEAVY ATOMS,  $R_L = 17.0a$



LIGHT ATOMS,  $R_L = 17.0a$



Comparison of the  $T=0$  LDA to the finite- $T$  QMC snapshot for the two cases with  $U=1$ :

$\omega=1/12.9$  (top)  
and  $\omega=1/17$   
(bottom).

Note the remarkable agreement.

# Local Density approximation

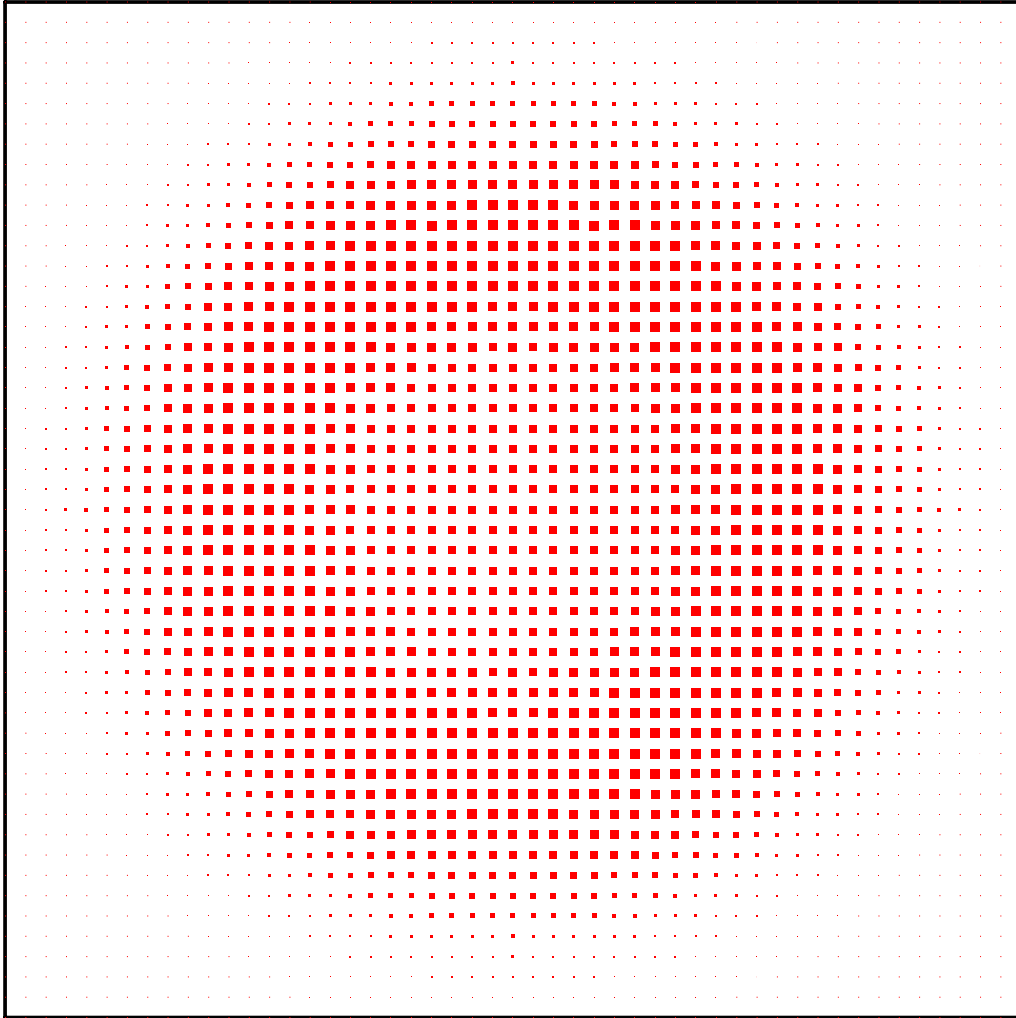
*Nonmonotonicity:* The local density approximation does not vary monotonically for the radial density of either atomic species or for the total density. This occurs due to the presence of ordered phases, which can break the nonmonotonic behavior. The curves for the light atom density are, of course, *piecewise monotonic* when the system is in one particular ordered phase and the chemical potential for the light atoms increases as we move outward in radius.

# Faceting and the inhomogeneous dynamical mean-field theory approach

# Inhomogeneous DMFT

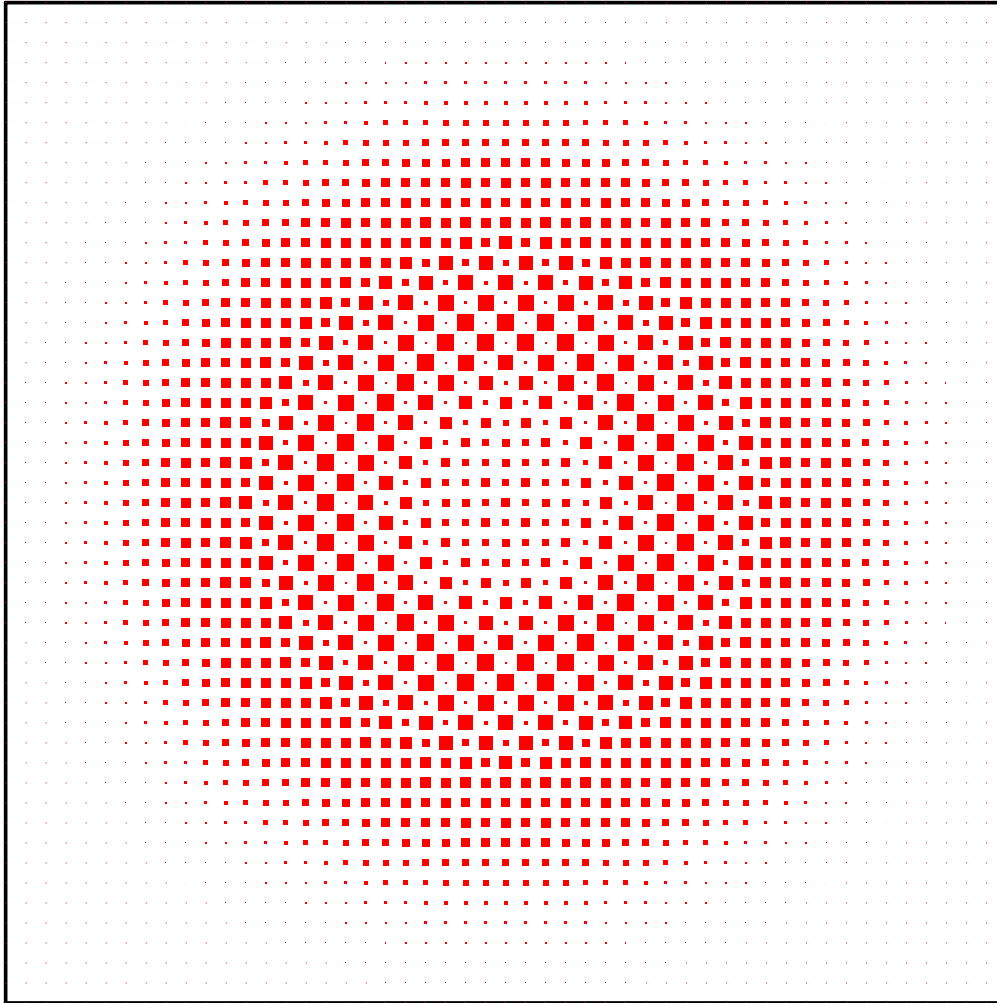
- Assume the self-energy is local, but can vary from one lattice position to another.
- The lattice Dyson equation needs to be solved in real space, but requires determining the diagonal of the inverse of a sparse matrix.
- Expect transition temperatures to be higher because of the neglecting of spatial fluctuations.

$U=1$ ,  $\omega_L=1/12.9$ , IDMFT approximation



$T=0.05$  no  
order seen.

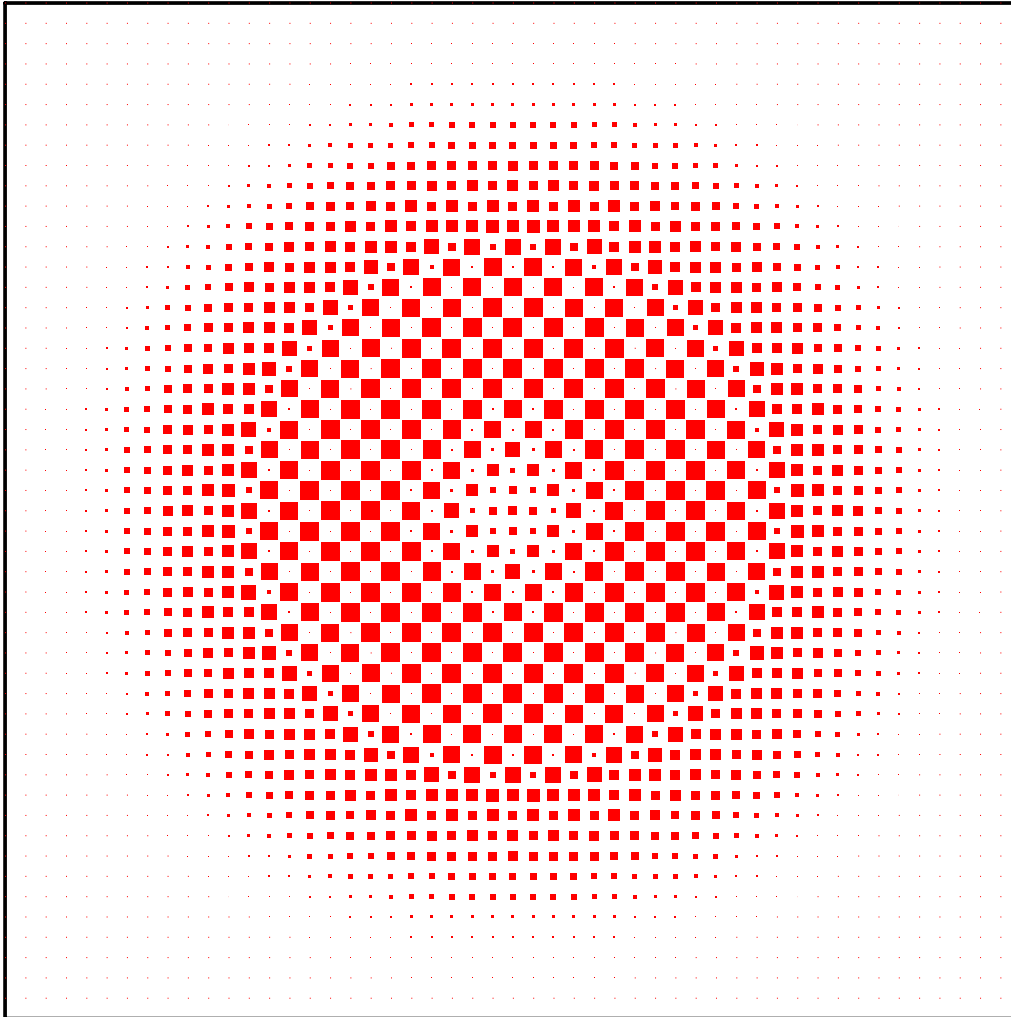
$U=1$ ,  $\omega_L=1/12.9$ , IDMFT approximation



$T=0.04$ ,  
checkerboard  
order begins  
in the high  
density ring.

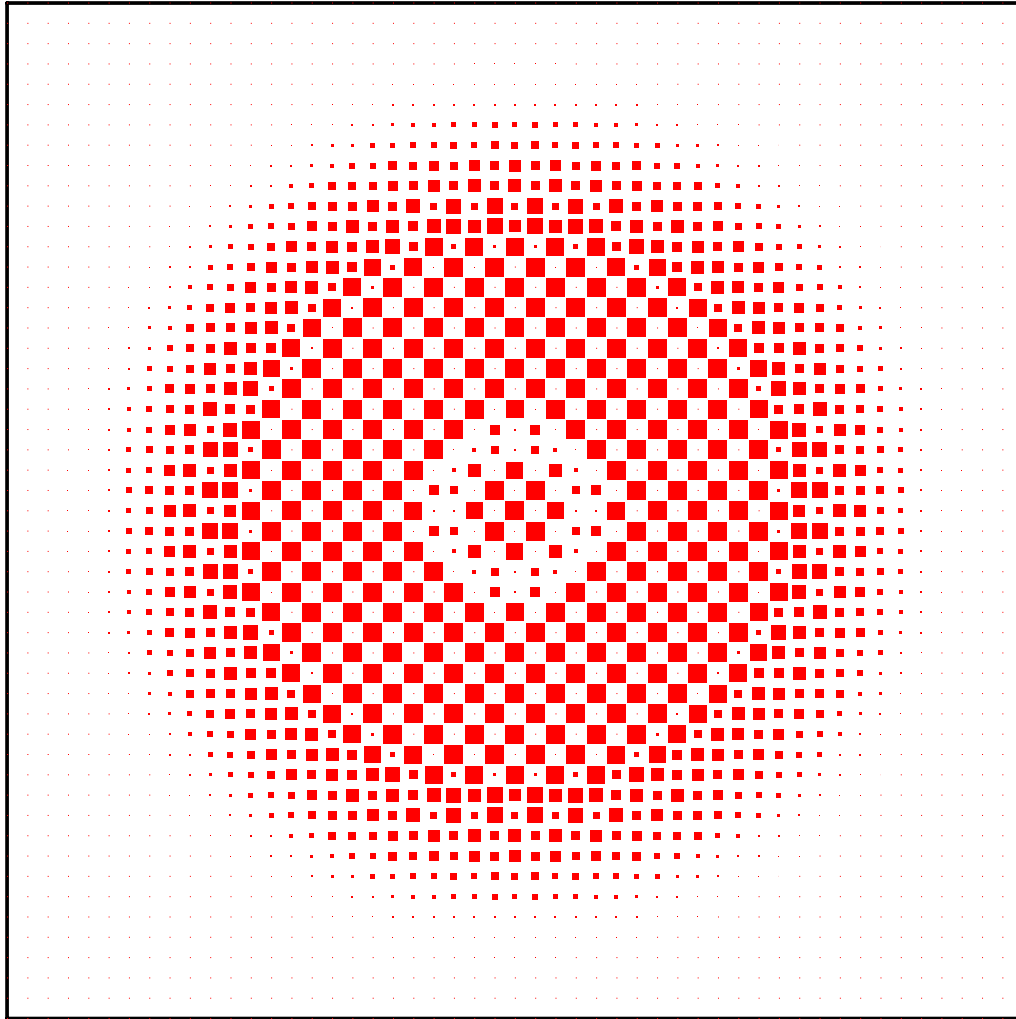


# $U=1$ , $\omega_L=1/12.9$ , IDMFT approximation



- $T=0.03$ , the annulus closes---note the faceting of the hole, and of the outer edge of the annulus.

# $U=1$ , $\omega_L=1/12.9$ , IDMFT approximation



- $T=0.02$ ;  
perhaps  
order  
nucleates in  
the center  
and pushes  
the  
disordered  
phase  
outward.  
(Results not  
converged  
yet).

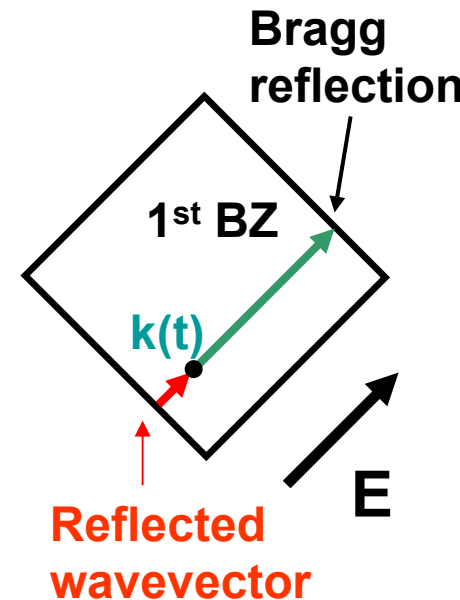
# Summary of pattern formation

- Pattern formation appears to be ubiquitous in mixtures of light and heavy fermionic atoms.
- Similar results to be expected if the heavy atoms are bosonic as well.
- Should be observable if one can get to the low temperatures needed to freeze in the ordered patterns.

# Nonequilibrium distribution functions for homogeneous systems in “pulled” optical lattices

# Atoms in a “pulled” lattice

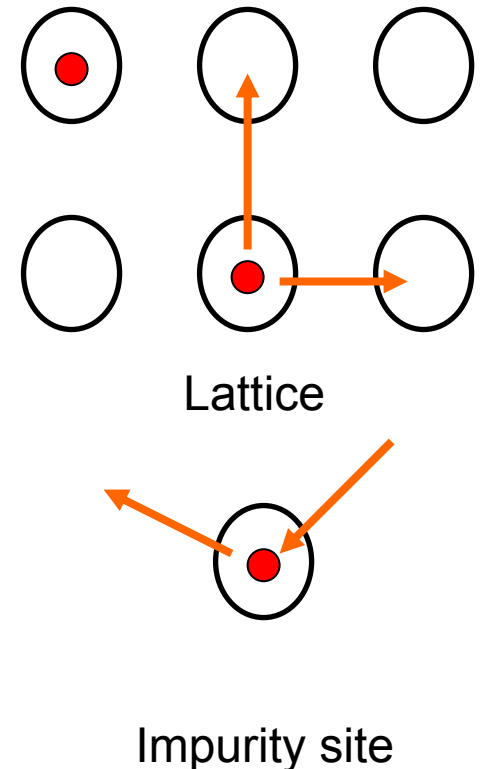
- In a **semiclassical** picture, the atomic momentum, written as  $\hbar\mathbf{k}=\mathbf{P}$ , evolves with a linear time-dependence corresponding to the **acceleration** due to the “field”:  $\mathbf{k}(t)=\mathbf{E}t$ .
- **Periodicity** modifies this picture: since the atoms are in a periodic optical lattice, the wavevector cannot increase **outside** of the first Brillouin zone; as it tries to move beyond the 1BZ it is **Bragg reflected** to the opposite side of the zone (so-called Bloch oscillations).
- Other atoms are sources of **scattering**, which also interrupt the evolution of the wavevector in the BZ.



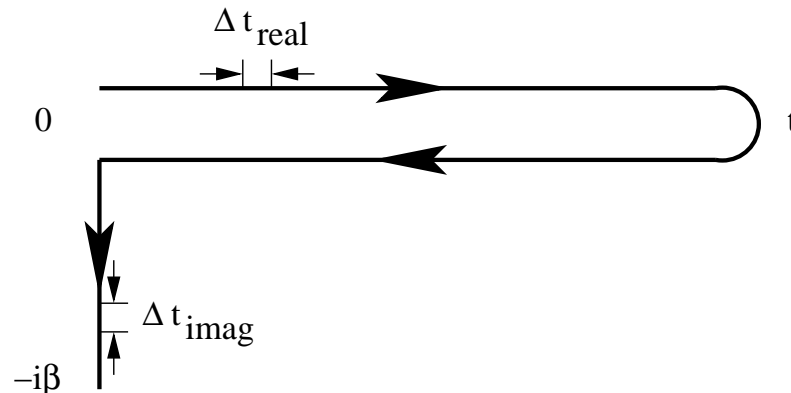
# Many-body physics and the dynamical mean-field theory approach to nonequilibrium problems

# Dynamical mean field theory

- Models of strongly correlated atoms are difficult to solve.
- Significant progress has been made over the past 18 years by examining the limit of **large spatial dimensions**.
- In this case, the lattice problem can be mapped onto a self-consistent impurity (single-site) problem, in a time-dependent field that **mimics the hopping of atoms onto and off of the lattice sites**.



# Kadanoff-Baym-Keldysh formalism



- Problems without time-translation invariance can be solved with a so-called **Keldysh formalism**.
- Green's functions are defined with time arguments that run over the **Kadanoff-Baym-Keldysh contour**.
- The atoms evolve in the fields **forwards** in time, then de-evolve in the fields **backwards** in time.
- **Functional derivatives** are then used to determine the Green's functions.



# Dynamical mean-field theory algorithm

**Dyson equation**

$$\Sigma = G_0^{-1} - G_{\text{loc}}^{-1}$$

**Hilbert transform**

$$G_{\text{loc}} = \sum_k [G_k^{\text{non}}(E) - \Sigma]^{-1}$$

**Dyson equation**

$$G_0 = (G_{\text{loc}}^{-1} + \Sigma)^{-1}$$

**Solve impurity problem**

$G_{\text{loc}} = \text{Functional}(G_0)$   
{example: FK model:  
 $G_{\text{loc}} = (1 - w_1)G_0(\mu) + w_1 G_0(\mu - U)$ }

All objects ( $G$  and  $\Sigma$ ) are **matrices** with each time argument lying on the contour.

# Pulled lattice and the generalized Hilbert transform

The band structure is a sum of cosines on a hypercubic lattice:

$$\varepsilon(k) = -\frac{t^*}{2\sqrt{d}} \sum_{i=1} \cos k_i \Rightarrow -\frac{t^*}{2\sqrt{d}} \sum_{i=1} \cos[k_i + E_i t] = \varepsilon \cos[Et] + \bar{\varepsilon} \sin[Et]$$

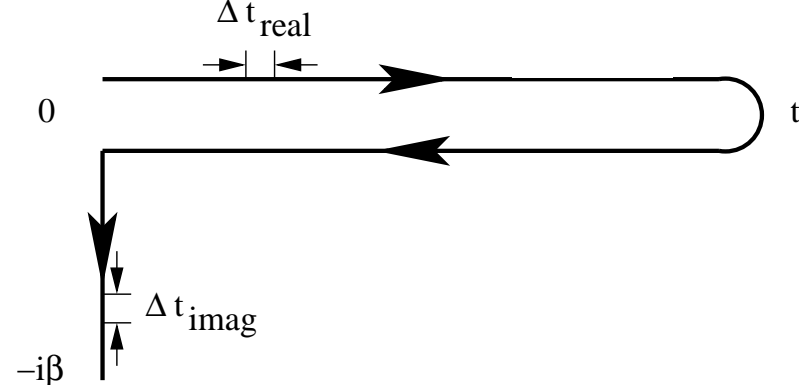
which becomes the sum of two “band energies” when the lasers are detuned so that the lattice is “pulled” in the diagonal direction.

These band energies have a joint Gaussian density of states, so a summation over the Brillouin zone can be replaced by a two-dimensional Gaussian integral.

We use about 100 Gaussian quadrature points *in each dimension* to perform the integration.

# Computational elements for a massively parallel solution of the many-body problem

# Computational elements



The key issue in calculating the real-time Green's function is to evaluate the **Dyson equation of a continuous integral operator** defined on the Kadanoff-Baym-Keldysh contour.

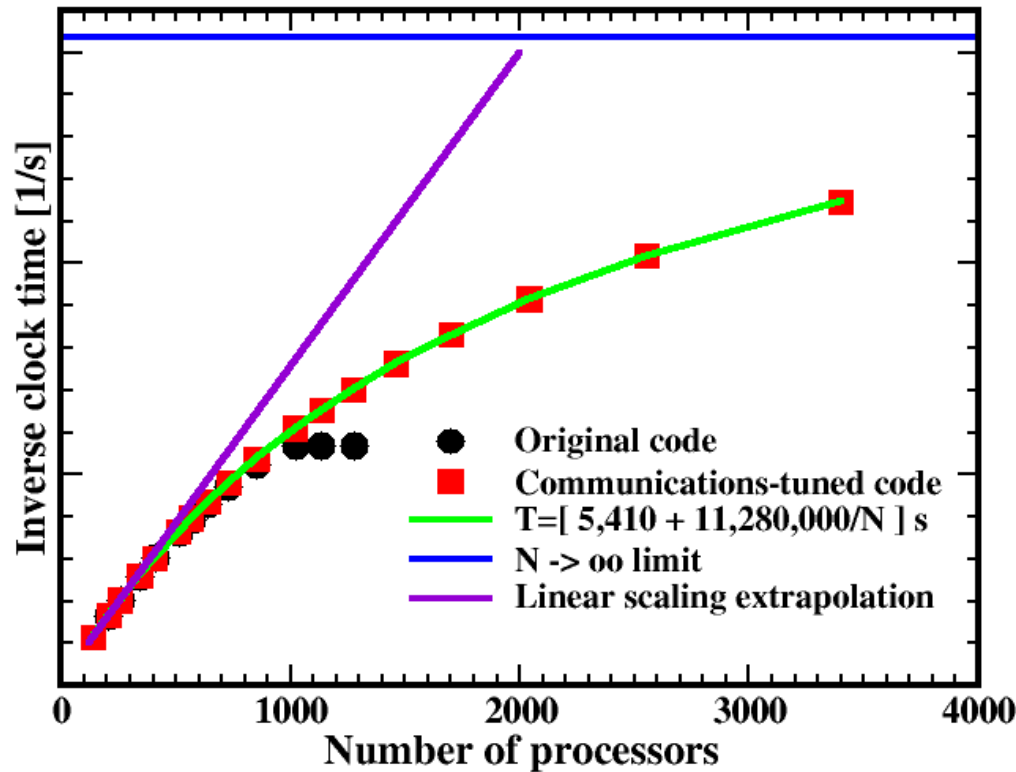
This operator is first **discretized** on a grid to be represented by **finite-dimensional** matrices.

Next, we need to integrate the dependence of the **matrix elements** over a **two-dimensional** energy space.

Each matrix element is constructed from **one matrix inverse** and **two matrix multiplications**. We typically work with (approximately 10,000) **general complex matrices** of size up to 5700X5700.

Since the only information needed to generate the matrices is the local self-energy matrix  $\Sigma$ , the electric field  $\mathbf{E}$ , and the temperature  $T$ , **this procedure is easily parallelized**.

# Scaling

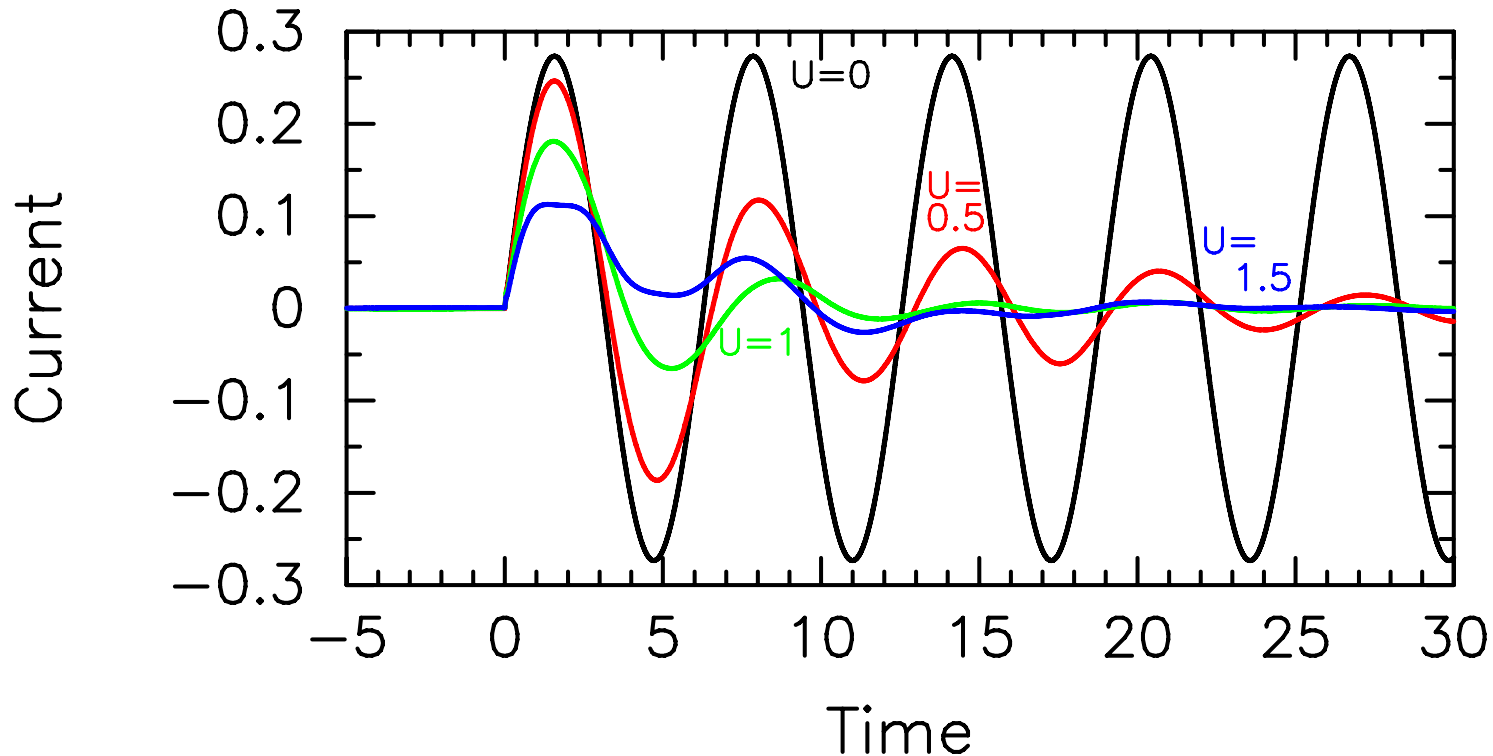


The algorithm has a natural parallelizable piece and a serial piece, so it can never achieve pure linear scaling for strong scaling. The green curve is the strong scaling prediction, red squares the actual data.

**When originally scaled, the data showed a bottleneck when increased beyond about 900 processors. This was a communications issue, resolved by removing many-to-one sends in the quadrature. Scaling is sublinear, but achieves about 70% of linear efficiency on 1500 procs.**

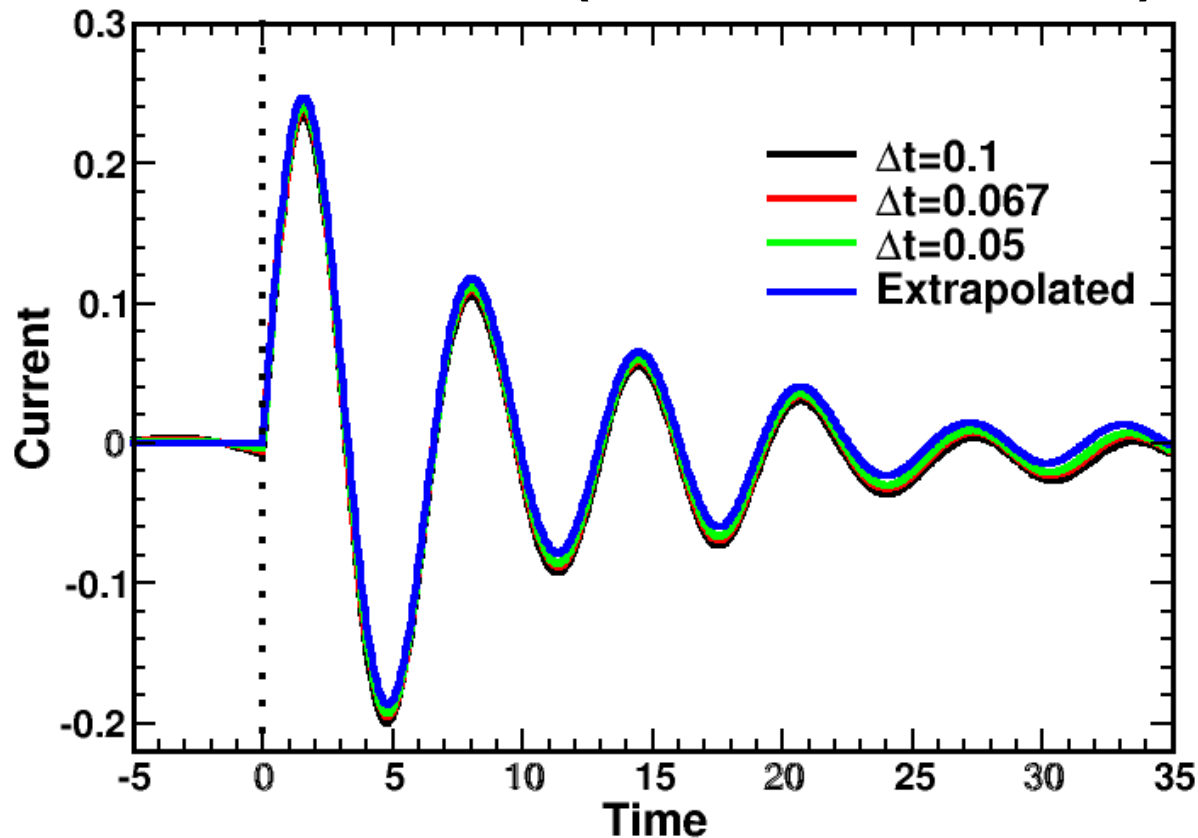
# Computational Results

# Bloch oscillations in conductors ( $E=1$ )



As the scattering increases, the amplitude of the current decays faster, but we cannot tell whether the oscillations survive at long time, or are completely damped.

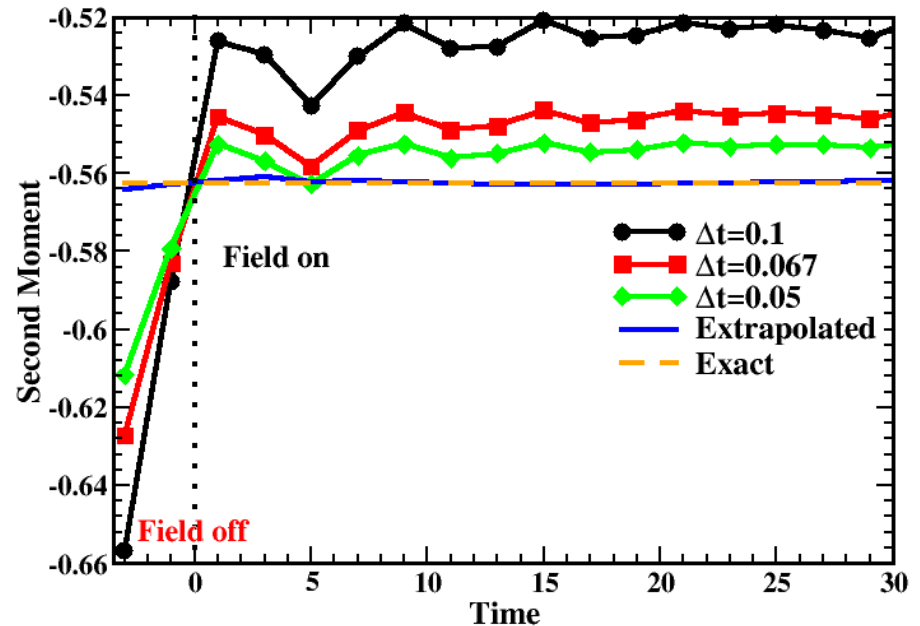
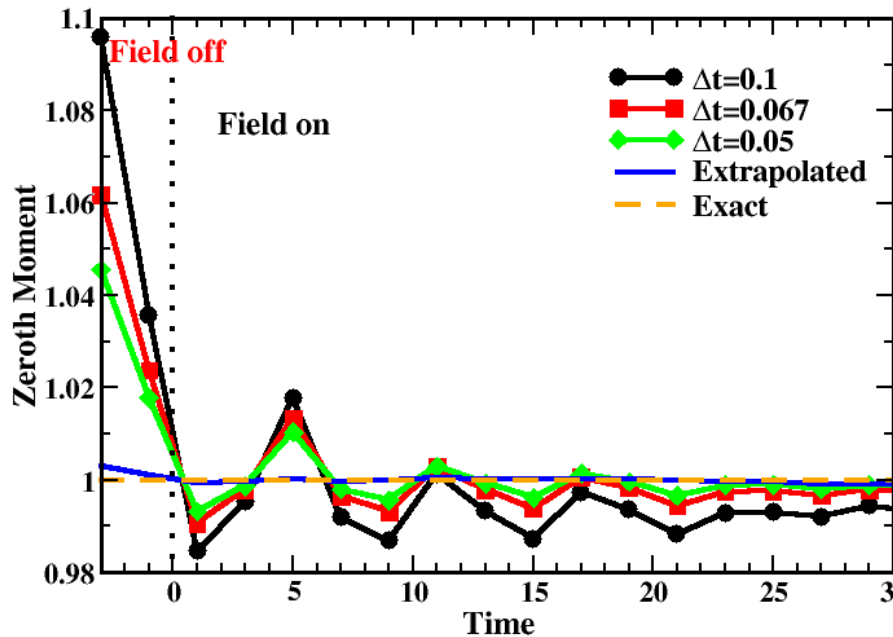
# Accuracy of results—scaling of the current ( $E=1$ , $U=0.5$ )



The accuracy of the current is illustrated here with a plot showing results for different discretizations and the extrapolated current.



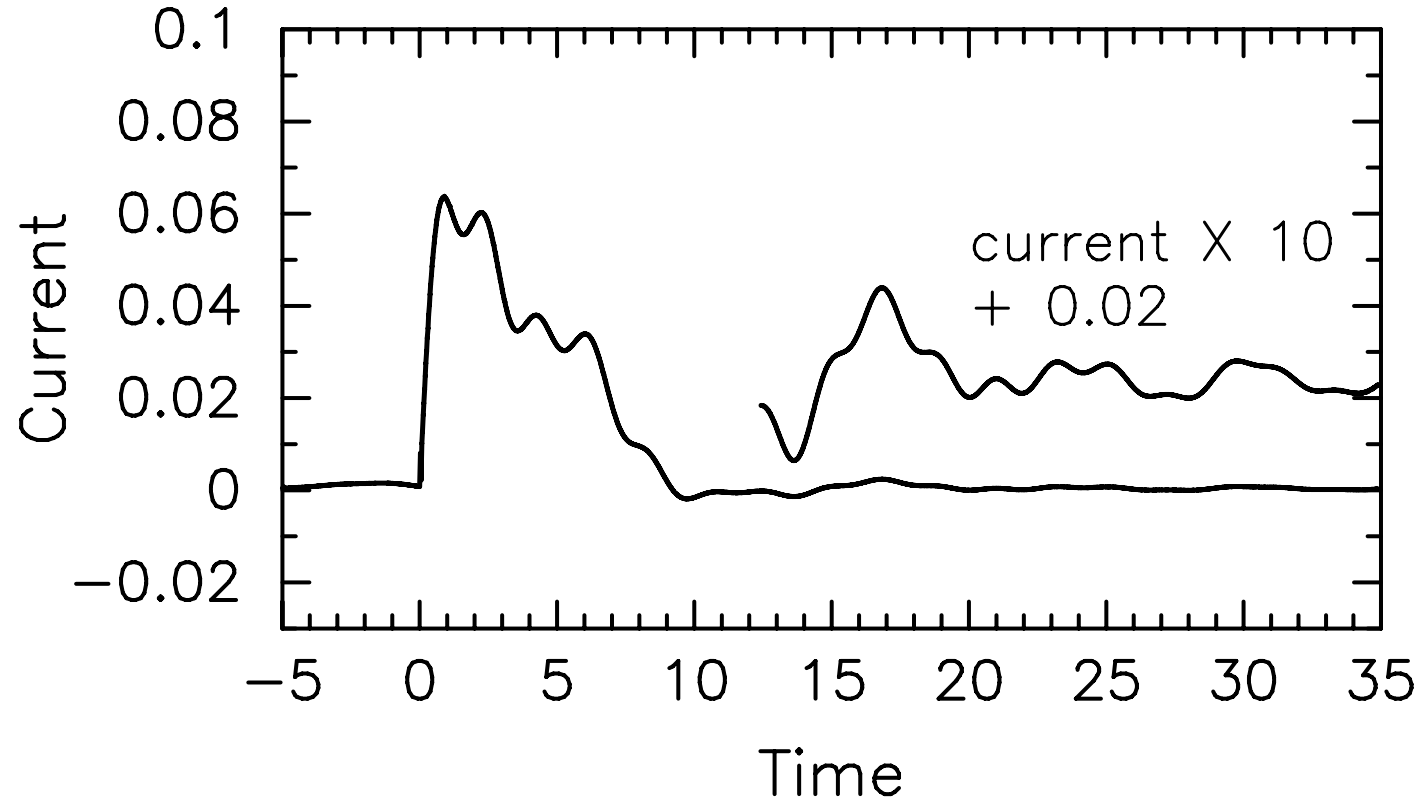
# Accuracy of the results---scaling of moments ( $E=1$ , $U=0.5$ )



**Exact results** are known for the equal time Green's functions and their first two derivatives.

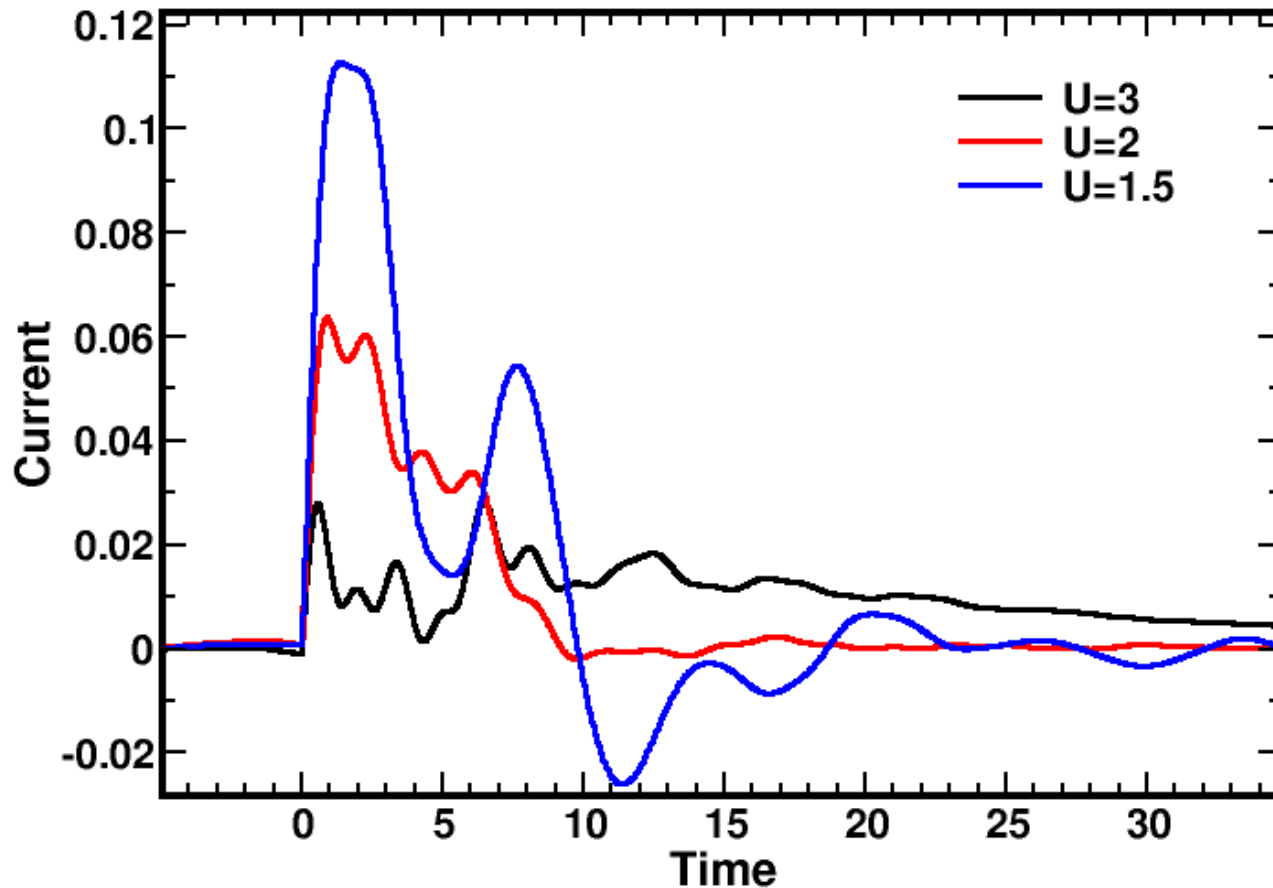
**Extrapolating** the results to zero discretization size yields **excellent agreement** with the exact results.

# Current in the Mott Insulator ( $E=1$ , $U=2$ )



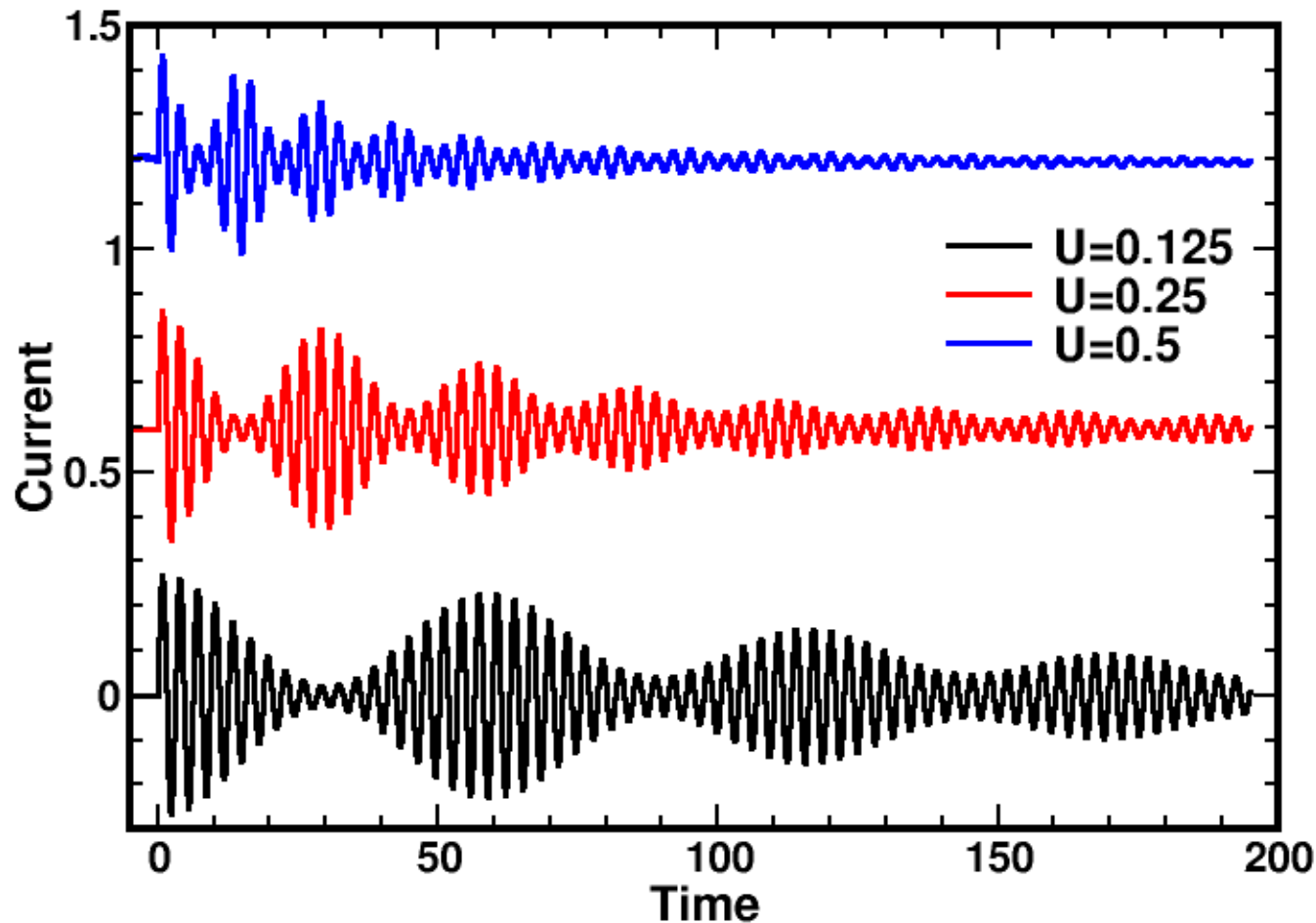
In the Mott insulator, the regular Bloch oscillations are replaced by irregular oscillations. Note that they survive out to long times (albeit with low amplitude).

# Current in the Mott Insulator ctd.



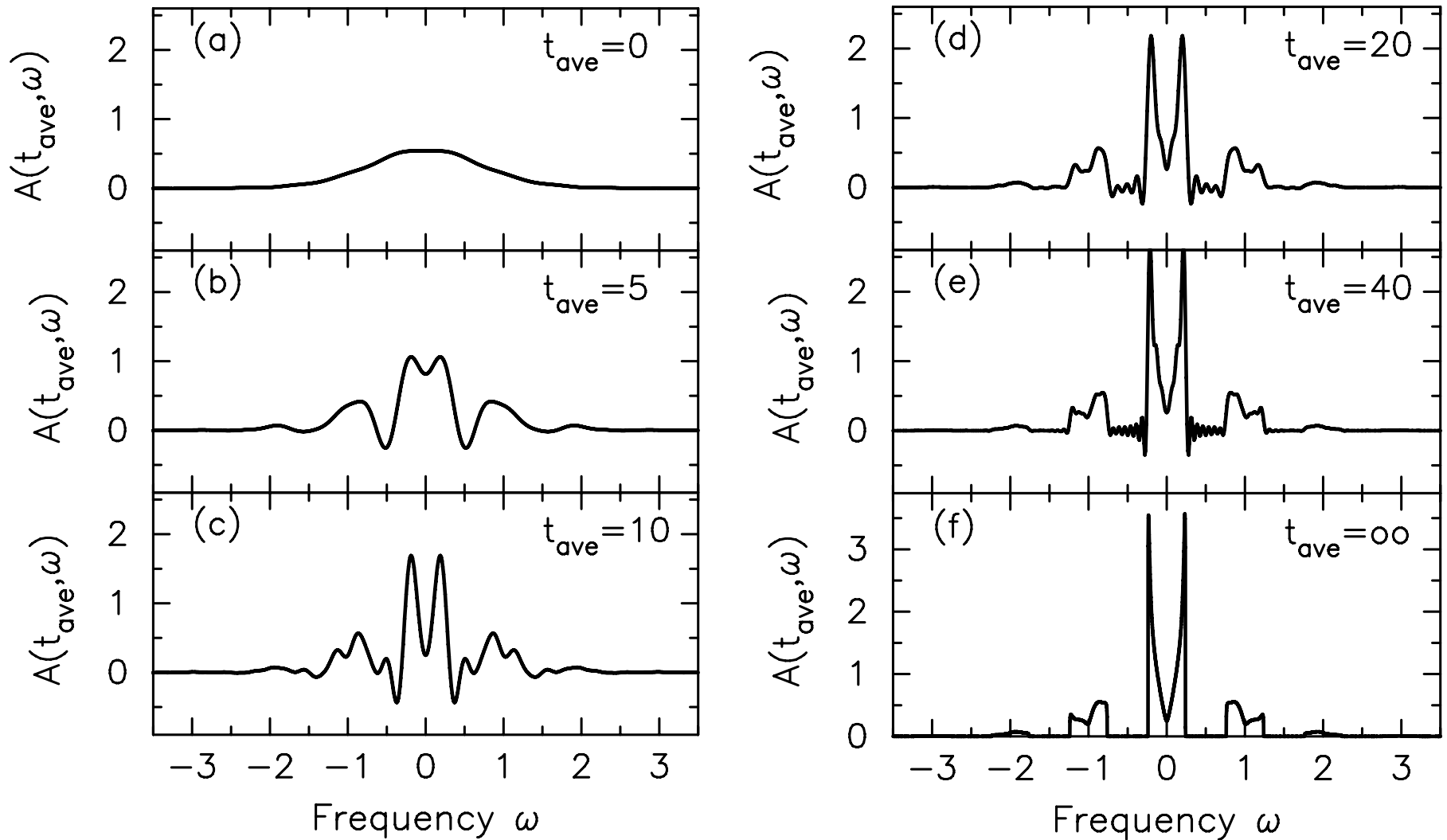
Notice how the oscillations change character from damped Bloch oscillations to irregular damped oscillations as the size of the gap in the Mott insulator increases.

# Beats in the current at large field

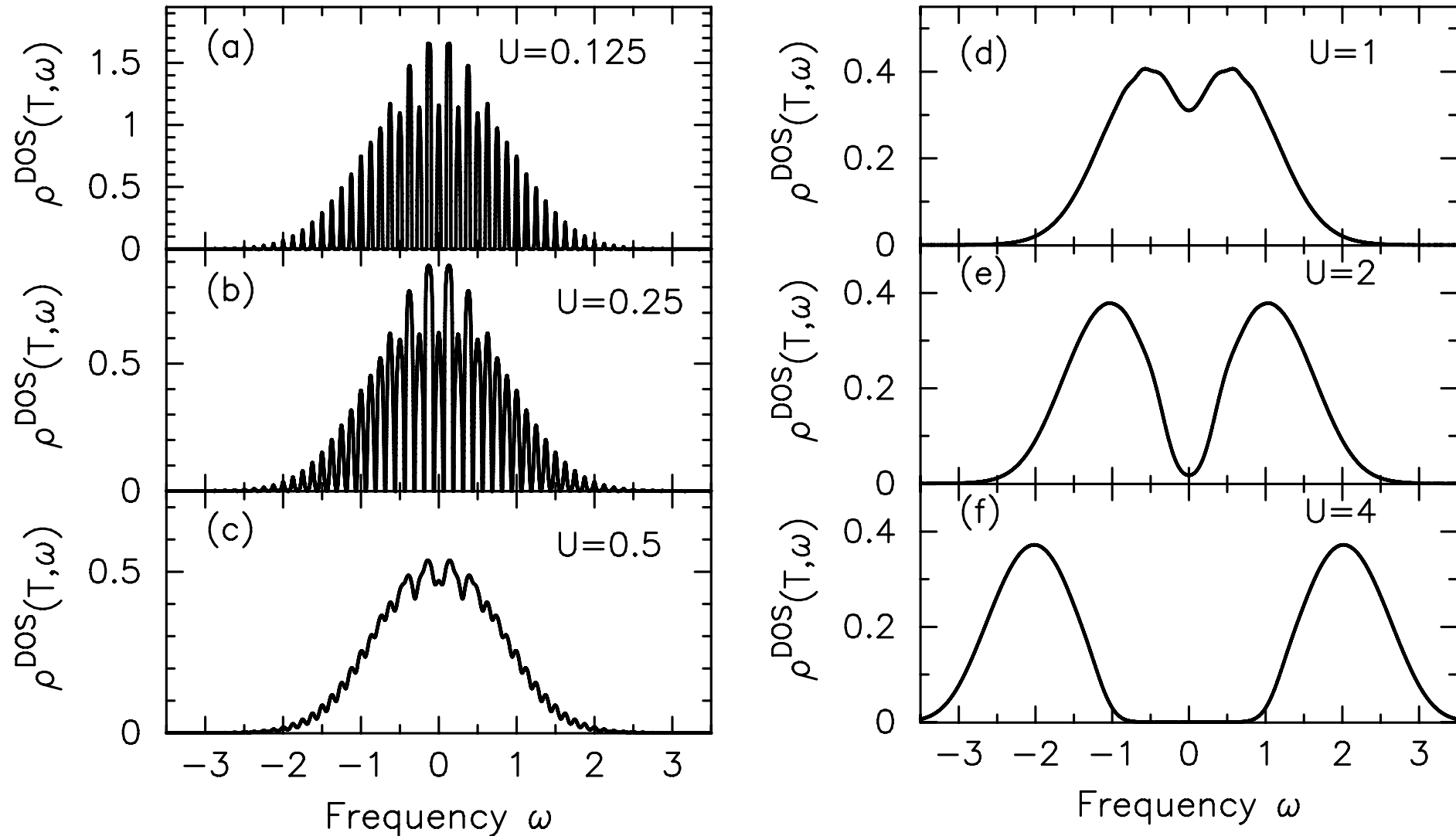


When the field is large ( $E=2$  here), near beats develop with a beat period proportional to  $1/U$ . The origin of the beats is a splitting in the DOS peaks by  $U$ .

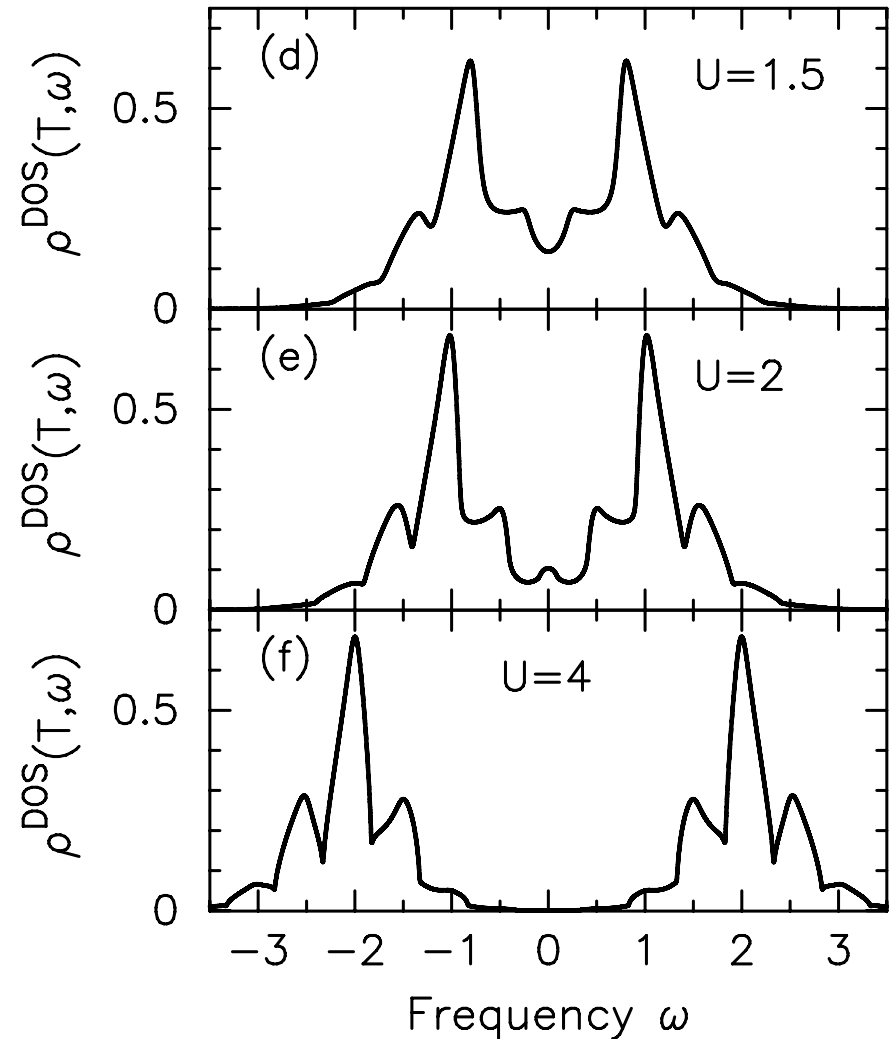
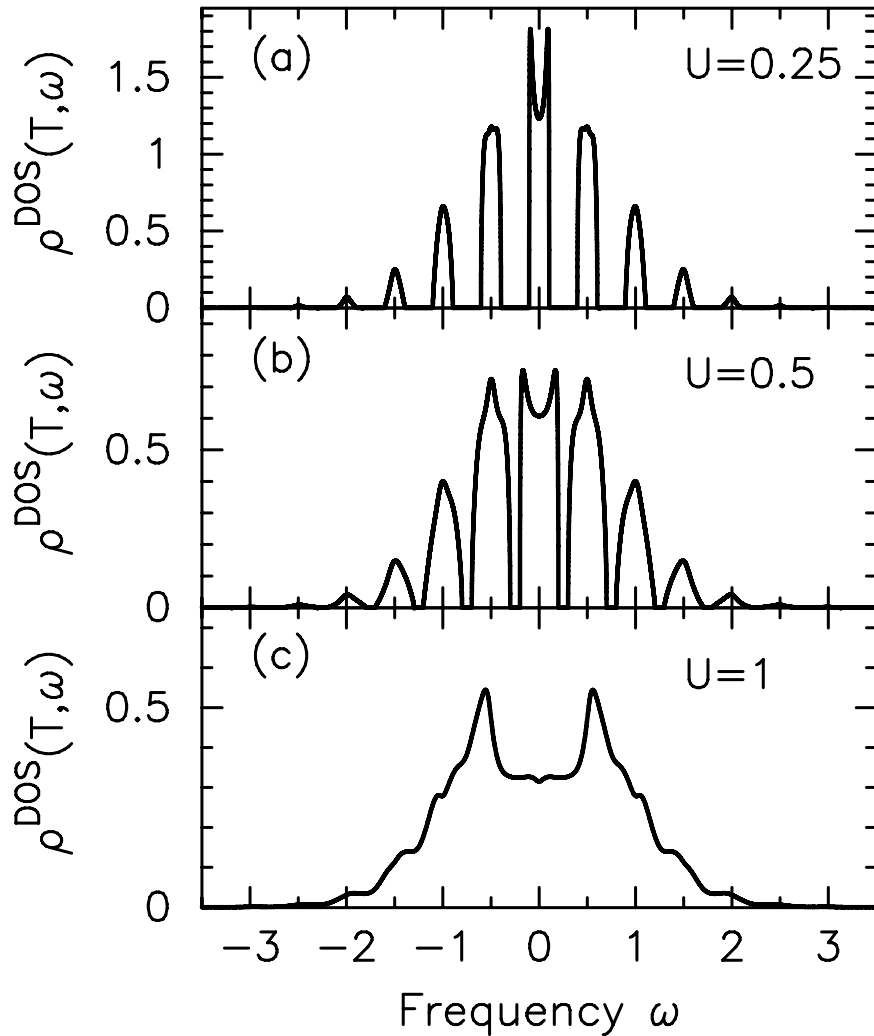
# Transient density of states ( $E=1$ , $U=0.5$ )



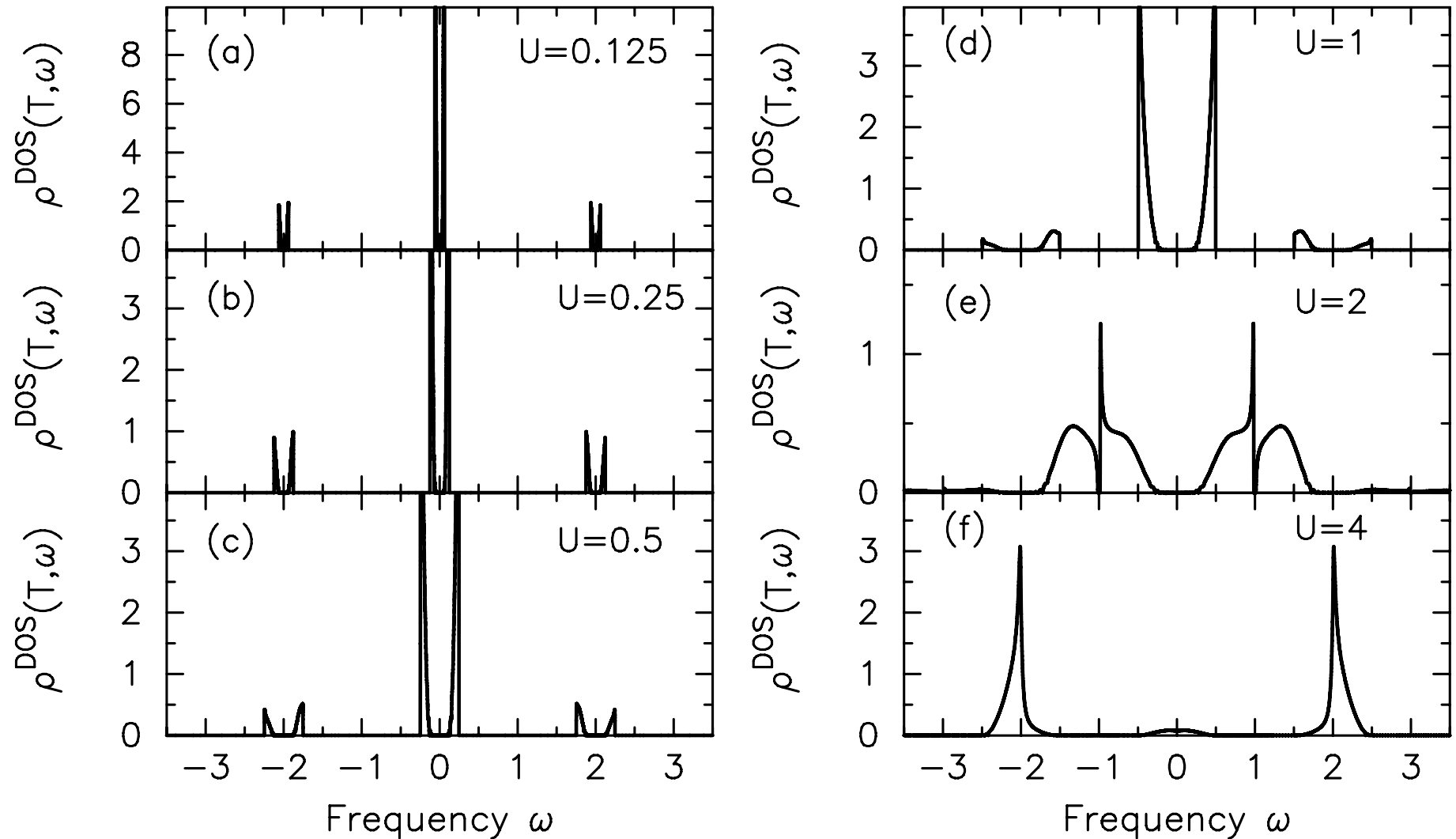
# Density of states ( $E=0.125$ )



# Density of states ( $E=0.5$ )



# Density of states ( $E=2$ )



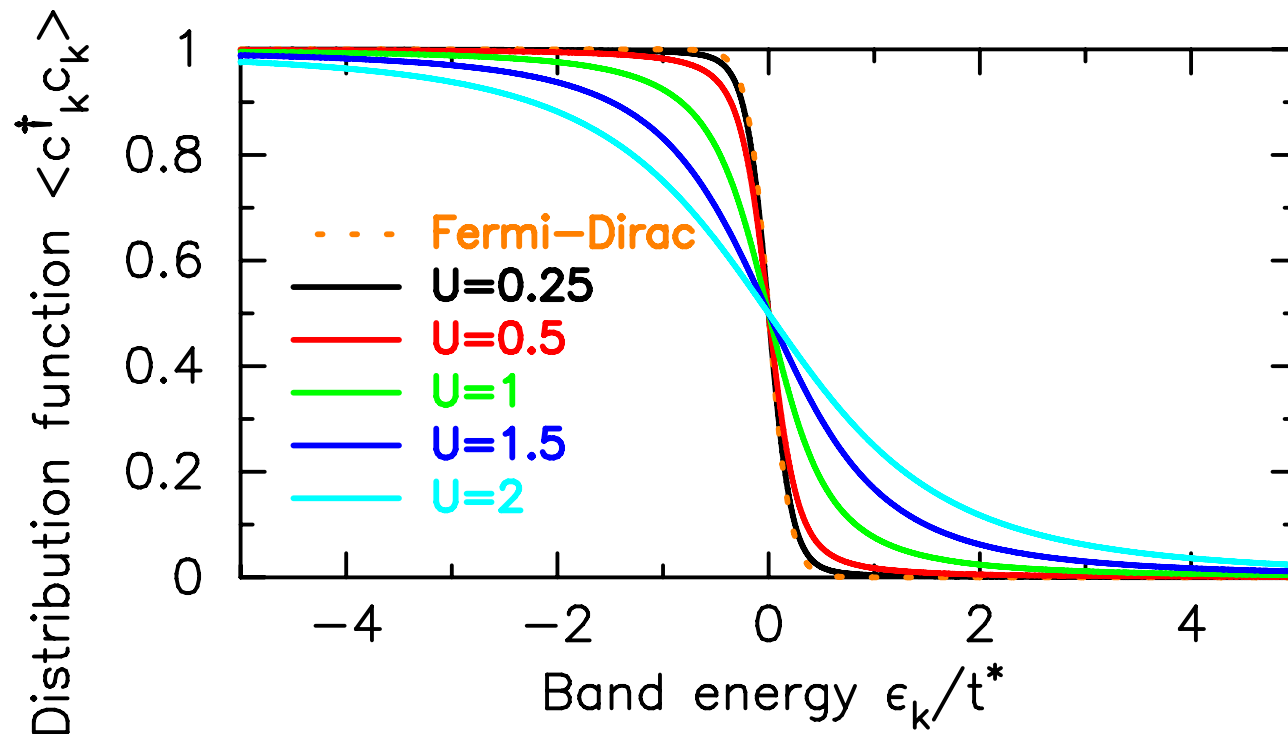


# Application to ultracold atoms

# Distribution function of the light atoms

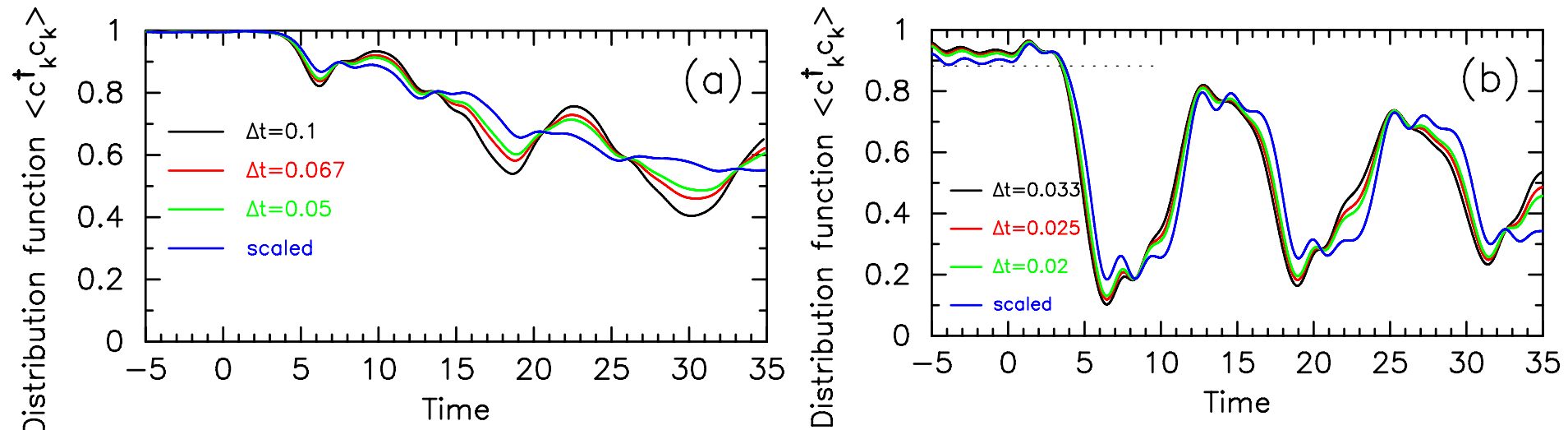
The distribution of the light atoms through the Brillouin zone can be measured via a time-of-flight experiment. Theoretically, it is given by the equal-time lesser Green's function. It may be necessary to average over numerous “shots” to create images appropriate for the annealed averaging over the heavy atomic positions.

# Equilibrium distribution function



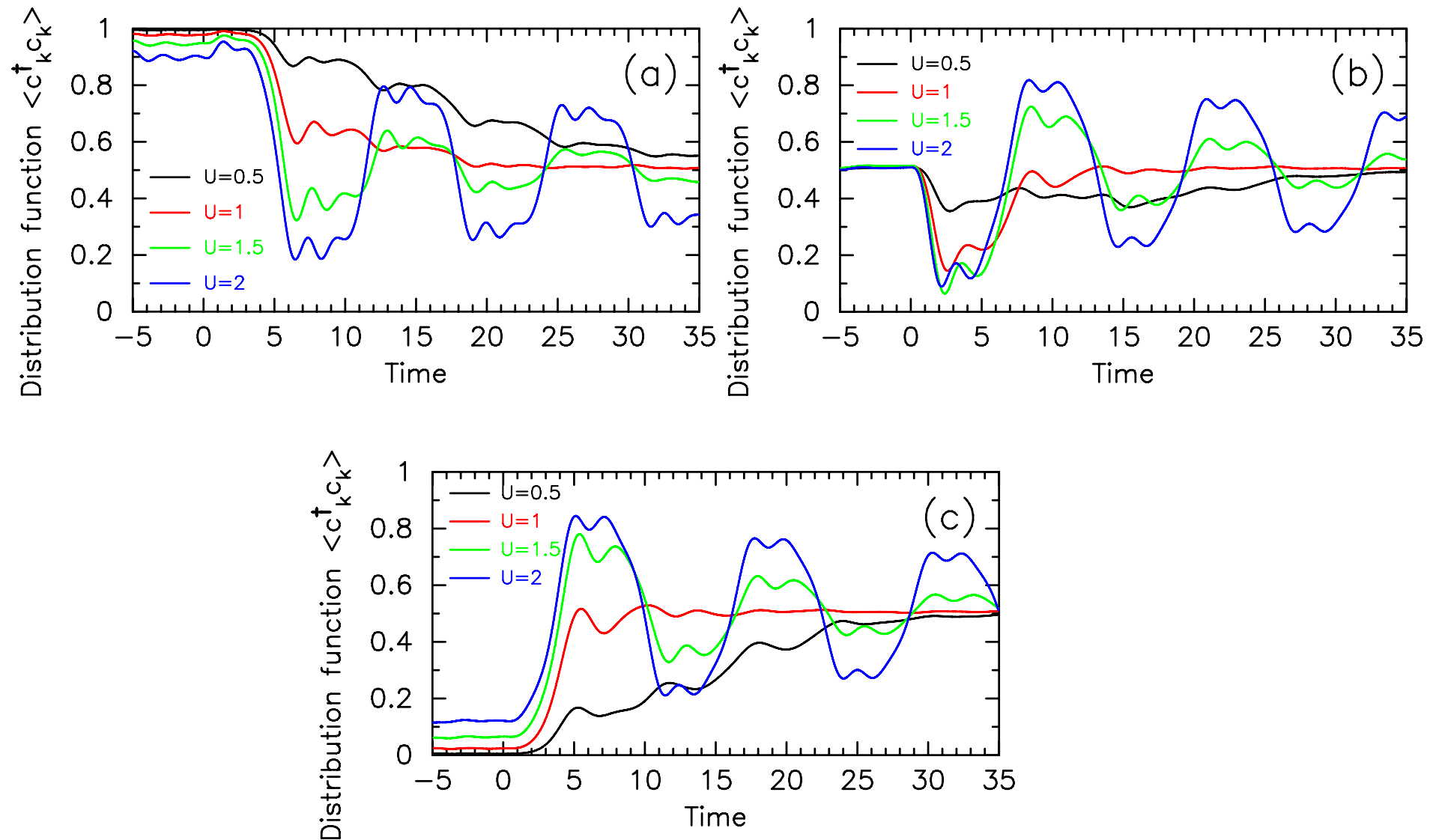
The equilibrium distribution function depends only on the band energy. It decreases in magnitude for negative energies as  $U$  increases.

# Scaling of distribution function

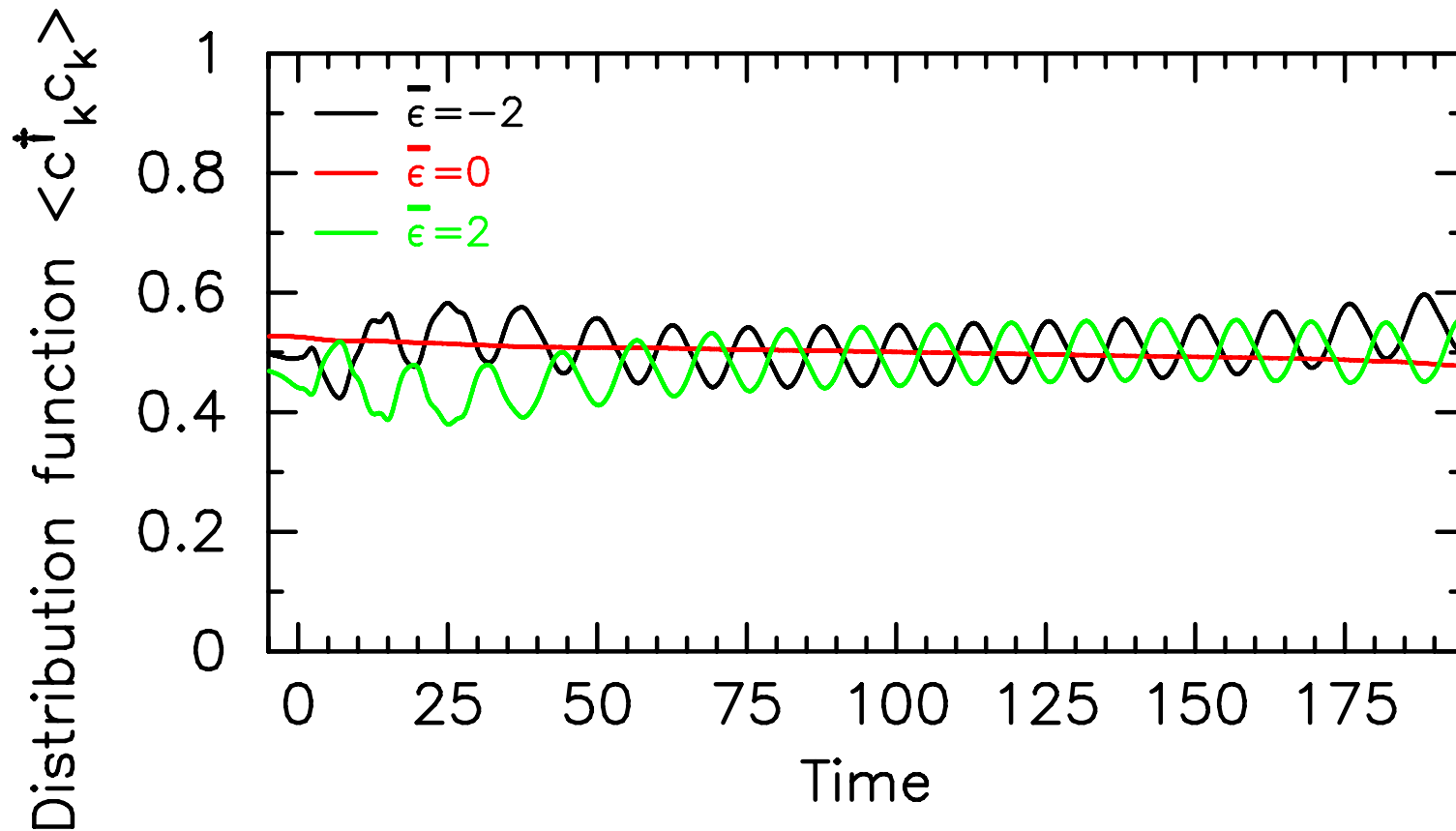


The distribution function scales well when we use a quadratic scaling for the three smallest discretization sizes. Left is  $U=0.5$  and right is  $U=2$ . This point in the BZ is  $\varepsilon=-2$  and  $\bar{\varepsilon}=-2$ .

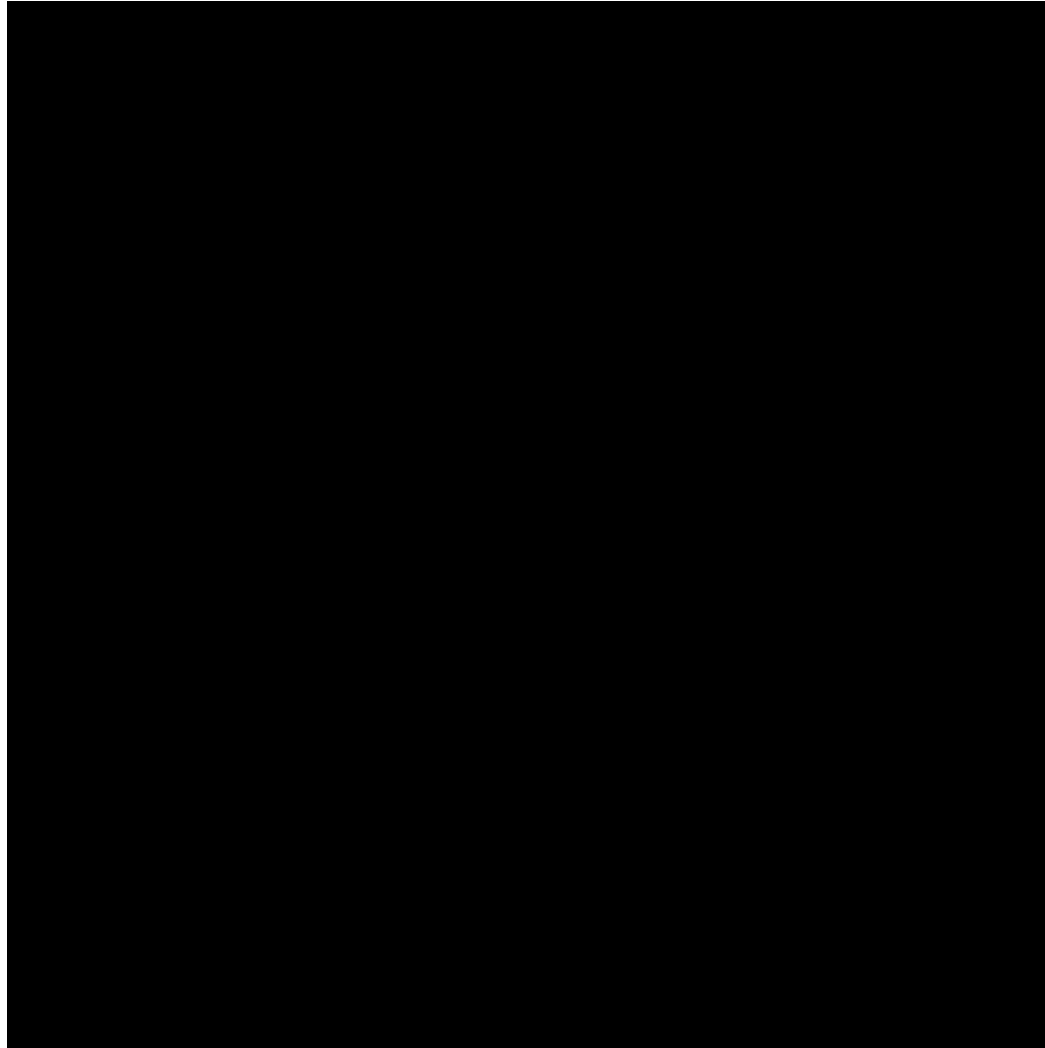
# Dependence on U



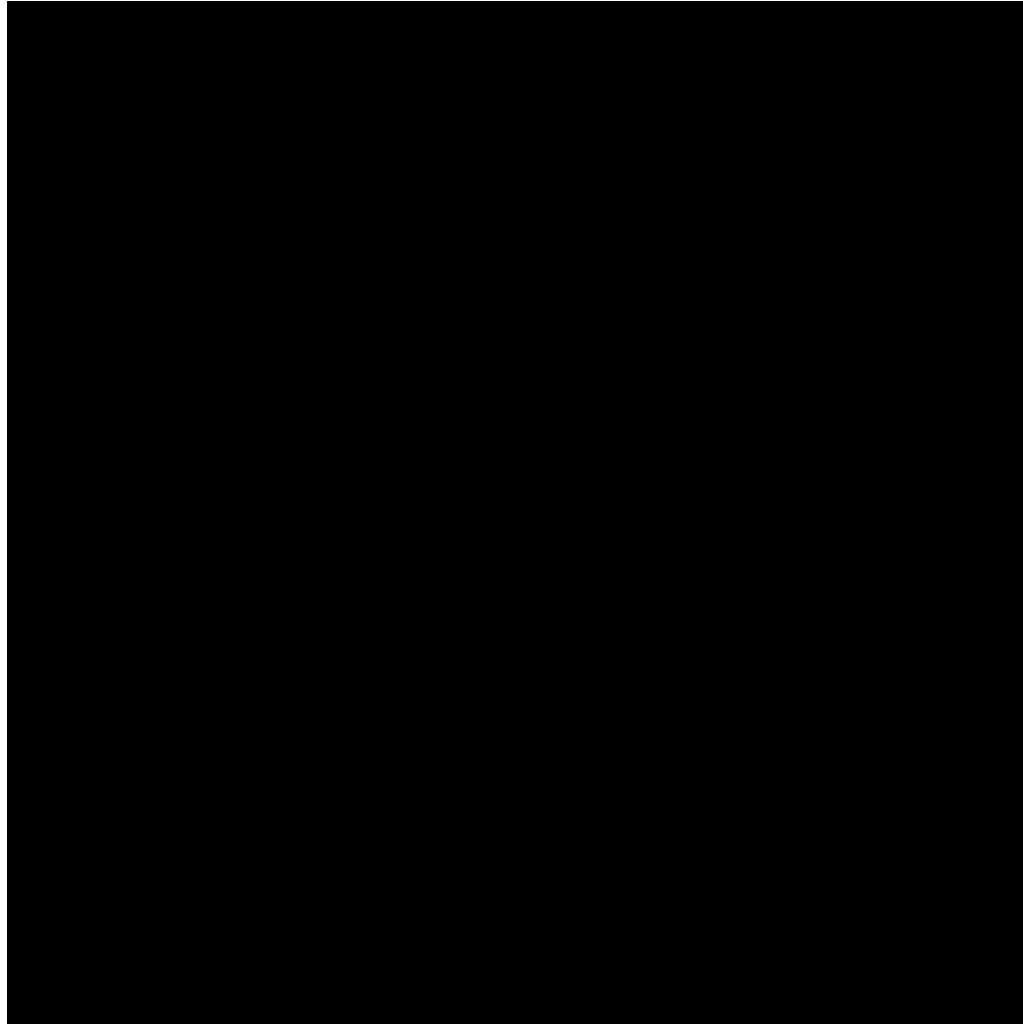
# Long-time oscillations



# Strongly scattering conductor ( $E=0.5$ , $U=0.5$ )

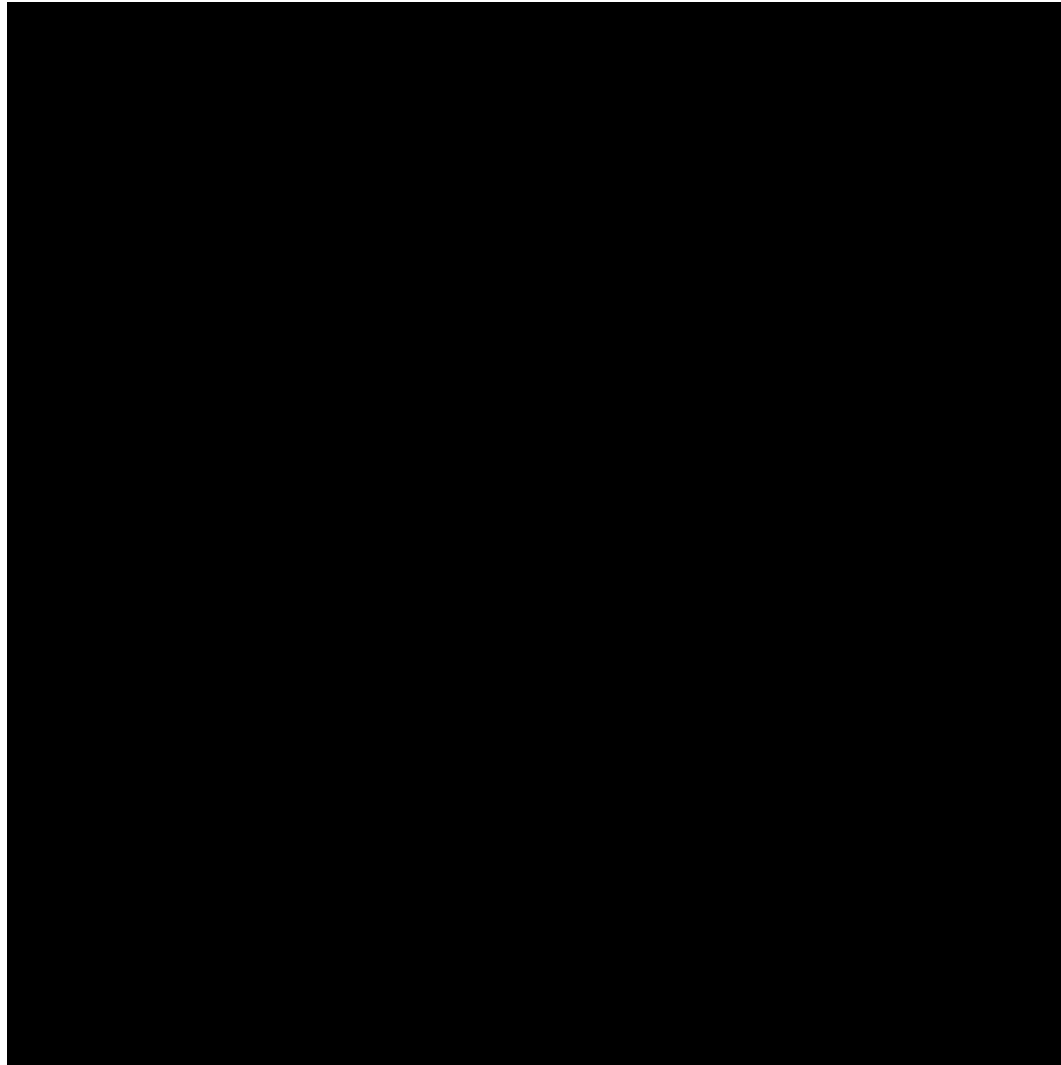


# Strongly scattering conductor ( $E=2$ , $U=0.5$ )

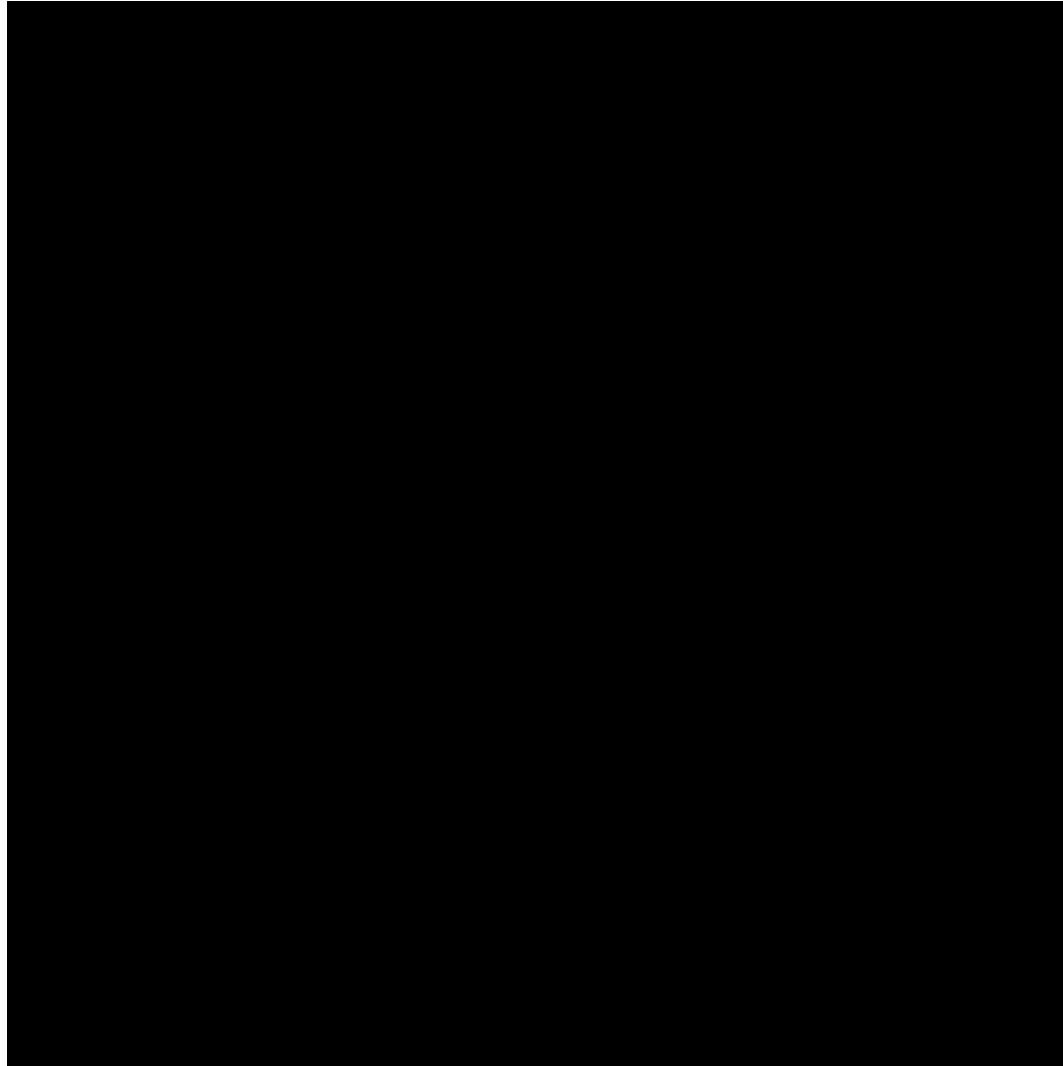




# Mott insulator ( $E=0.5$ , $U=1.5$ )



# Mott insulator ( $E=2$ , $U=1.5$ )



# Conclusions

- Illustrated a range of complex phenomena that can occur in cold atom mixtures of fermionic atoms with different masses.
- Pattern formation shows both labyrinthine patterns and ordered geometrical phases.
- By pulling the lattice in a particular direction, one can generate a nonequilibrium distribution of the atoms, which illustrate complex evolutions in time.